Chinese Chemical Letters 35 (2024) 109007

Contents lists available at ScienceDirect

Chinese Chemical Letters

journal homepage: www.elsevier.com/locate/cclet

Activation of biomass-derived porous carbon for supercapacitors: A review

Zixuan Guo[a], Xiaoshuai Han[a], Chunmei Zhang[b,*], Shuijian He[a], Kunming Liu[c], Jiapeng Hu[d], Weisen Yang[d], Shaoju Jian[d], Shaohua Jiang[a,*], Gaigai Duan[a,*]

[a] Jiangsu Co-Innovation Center of Efficient Processing and Utilization of Forest Resources, International Innovation Center for Forest Chemicals and Materials, College of Materials Science and Engineering, Nanjing Forestry University, Nanjing 210037, China
[b] Institute of Materials Science and Devices, Suzhou University of Science and Technology, Suzhou 215009, China
[c] Faculty of Materials Metallurgy and Chemistry, Jiangxi University of Science and Technology, Ganzhou 341000, China
[d] Fujian Provincial Key Laboratory of Eco-Industrial Green Technology, Key Laboratory of Green Chemical Technology of Fujian Province University, College of Ecological and Resources Engineering, Wuyi University, Wuyishan 354300, China

ARTICLE INFO

Article history:
Received 11 July 2023
Revised 11 August 2023
Accepted 28 August 2023
Available online 30 August 2023

Keywords:
Biomass-derived
Activation
Pore structure
Electrochemistry
Supercapacitor

ABSTRACT

Due to the advantages of renewable, low pollution and wide distribution of biomass resources, it is selected as the electrode material for supercapacitors. For carbon-based electrode materials, specific surface area and pore structure have a great influence. Exploring and summarizing the influence of activation on pore structure will greatly broaden this field. Based on the activation mechanism of activator, this paper summarizes the latest progress of biomass activation applied to supercapacitors, including traditional physical and chemical activation methods and non-traditional methods such as biological activation method, self-activation method, template assisted activation method and green activator activation. Finally, the challenges, strategies and prospects for the future development of biomass-derived carbon material activation are pointed out. In summary, this review will help researchers choose appropriate strategies to design biomass-derived carbon electrode materials for supercapacitors, thereby promoting the application of biomass materials.

1. Introduction

As an important material basis for human survival and development, fossil energy supports the progress of human civilization and the development of economy and society in the past two hundred years [1]. The large consumption of human beings and the non-renewable fossil energy leads to the emergence of energy crisis. Energy storage has become a great challenge for human beings in the 21st century. It is determined to develop energy storage devices with low cost, low carbon emission and environmental protection [2–5]. Supercapacitors can be traced back to the 1970s [6]. They have a larger specific surface area, and their capacitance is greatly improved compared with the traditional ones. They have fast charge and discharge speed, long cycle life, high power density, low environmental pollution, and wide operating temperature range [7]. Supercapacitors are composed of electrodes, electrolyte solutions, separators, and current collectors. According to the energy storage mechanism, supercapacitors can be divided into electric double layer supercapacitors, pseudocapacitance supercapacitor, and hybrid supercapacitors. There is no chemical reaction in the electric double layer supercapacitor. When two electrodes are inserted into the electrolyte at the same time and a voltage smaller than the decomposition voltage of the electrolyte solution is applied between them, the positive and negative ions in the electrolyte will move rapidly to the two poles under the action of the electric field, and form a close charge layer on the surface of the two electrodes respectively, relying on the electrostatic adsorption of ions occurring simultaneously at the positive and negative poles for energy storage. Pseudocapacitive supercapacitors undergo potential deposition through electroactive substances, and reversible chemical adsorption, desorption or redox reactions occur not only on the surface of the electrode, but also inside the entire electrode. Therefore, they can obtain higher capacitance and energy density than electric double layer capacitors. The formation of hybrid supercapacitors originates from the coupling of different redox pseudocapacitive materials (such as metal oxides and conductive polymers) and electric double layer materials (such as graphene and activated carbon). The energy storage principle depends on the

* Corresponding authors.
E-mail addresses: cmzhang@usts.edu.cn (C. Zhang), shaohua.jiang@njfu.edu.cn (S. Jiang), duangaigai@njfu.edu.cn (G. Duan).

https://doi.org/10.1016/j.cclet.2023.109007
1001-8417/

combination of electric double layer and pseudocapacitive energy storage mechanism. The performance of the supercapacitor is related to the electrode material, the electrolyte and the separator used, and the electrode material is the key to determine the capacitance performance. Because it is an important support for supercapacitors, the performance of electrode materials directly affects the performance of capacitors. At present, there are three main types of materials as supercapacitor electrodes: carbon materials, metal oxides and conductive polymers [8–12]. Carbon-based electrode has the advantages of low cost, good conductivity and good stability. With the increasing demand for human survival and development, it is urgent to seek a renewable energy to replace traditional fossil energy. Biomass has great potential as the only energy source that can replace fossil fuels under current energy constraints. Bilgili *et al.* [13] proposed several advantages of these promising biomass energy: (1) Good technical and economic credibility; (2) Abundant reserves; (3) Biomass resources help to solve energy dependence and national energy security problems by minimizing energy demand; (4) Biomass reduces poverty by improving the agricultural economy, increasing employment in rural areas. It promotes economic growth by developing industry. Therefore, developed countries tend to promote the use of biomass; (5) Biomass is effective in solving global problems such as global warming, climate change, air pollution and acid rain.

Biochar is generally prepared by carbonization of photosynthetic organic agricultural and forestry wastes (such as straw [14], grape [15], chestnut [16], wood [11,17,18], wheat bran [19], fruit core [16], and pollen [20]). The prepared biomass-derived carbon material is a widely used supercapacitor electrode material, which has the advantages of large specific surface area, developed pore structure, excellent conductivity, light weight and low cost [21–23].

The preparation of biomass porous carbon materials mainly includes: first, the raw materials are screened, and the required materials are finally prepared by high temperature carbonization and activation after pretreatment. Among them, activation refers to the reaction between biomass raw materials or precursors and activators, which causes partial carbon atoms to ablate and gasify, resulting in a large number of pores. The original pores will further expand, and even merge between pores, resulting in more complex pore structure of the material. Activation is the key to regulate the pore structure of carbon materials, which will directly affect the electrochemical and adsorption properties of porous carbon materials. Biochar has a variety of pore size distribution, including macropores (pore size greater than 50 nm), mesopores (pore size 2–50 nm) and micropores (pore size less than 2 nm) [24]. A large number of micropores provide abundant accumulation space for electrons, and play an important role in the adsorption/desorption process of charge through controlled diffusion and molecular sieve effect. Both macropores and mesopores provide channels for the transport of ions and charges. The mesopores shorten the diffusion distance of ions and reduce the diffusion resistance, so that ions can easily penetrate into the internal micropores. The large channel acts as a buffer ion storage layer, which helps the ion transport [25,26]. Improper pore structure matching of carbon materials will directly lead to the blockage of ion transport channels and low charge and discharge performance at high current [27]. Regulating the porosity and structure of biochar materials can improve the transmission efficiency of electrolyte ions, which is of great significance for improving the electrochemical performance of electric double layer supercapacitors. Therefore, it is necessary to study the activation mechanism during the preparation of porous carbon.

In this paper, the activation methods applied to the preparation of biomass porous carbon in recent years are summarized as shown in Fig. 1, including traditional physical activation, chemical activation and some unconventional activation methods. The action principle and future development direction of activators are systematically reviewed.

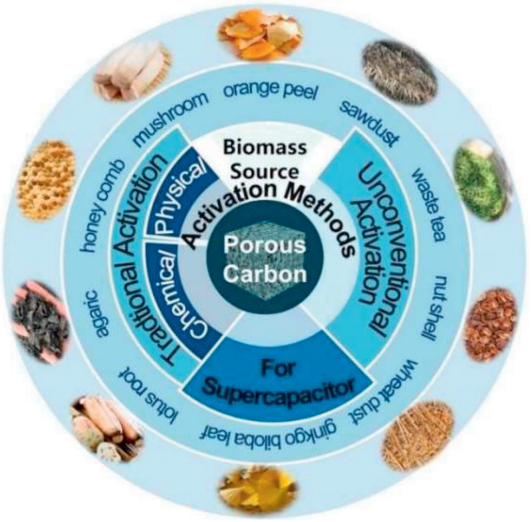

Fig. 1. An overview of activation of biomass-derived porous carbon for supercapacitor.

2. Traditional activations

The traditional activation methods of biomass porous carbon are mainly divided into physical activation and chemical activation.

2.1. Physical activation

Physical activation method refers to a method that uses oxygen containing gas such as water vapor, flue gas or air as an activator to react with atoms inside carbon materials at high temperatures. Physical activation can be divided into three steps: First, the removal of clogged adsorption media; Secondly, the pores formed in the precursor material are expanded; Finally, new pores are formed by selective oxidation of the carbon precursor.

With the official launch of the carbon market, the management of carbon dioxide emissions has become more stringent, and the resource utilization of carbon dioxide has gradually received attention. CO_2 can be used as an activator. When CO_2 diffuses into the pores and is adsorbed on the active sites of biochar, partial gasification occurs. The activation mechanism is as follows:

$$C_{active} + CO_2 \rightleftharpoons C_{active}\,(CO_2) \quad (1)$$

$$C_{active}\,(CO_2) \rightleftharpoons C_{active}\,(O) + CO \quad (2)$$

$$C_{active}\,(O) \rightleftharpoons CO \quad (3)$$

$$C_{active}\,(O) + CO \rightleftharpoons C_{active}\,(CO_2) \quad (4)$$

Rawat *et al.* [28] prepared biochar from litchi seeds and studied its application in supercapacitor electrodes. A symmetric supercapacitor using biochar obtained at 700 °C achieved a specific capacitance of 190 F/g at a current density of 1 A/g. After CO_2 activation, the capacitance increased significantly to 493 F/g. The charge-discharge cycle stability of the activated biochar supercapacitor is well maintained, and the capacitance retention rate is higher than

90% after 10,000 charge-discharge cycles in 1 mol/L H_2SO_4 electrolyte. The energy and power density of the water-based symmetric supercapacitor prepared using activated biochar are 24.6 Wh/kg and 0.6 kW/kg, respectively. Murugan Vinayagam *et al.* [29] took Syzygium cumini fruit shells (SCFS) and Chrysopogon zizanioides roots (CZR) as raw materials, carbonized them and placed them in a tube furnace, and then injected CO_2 into N_2 atmosphere for activation. SCFS carbon source samples showed microporous characteristics, while CZR carbon source samples showed mesoporous characteristics. The formation of CSR-AC mesopores was attributed to the higher ash content of CZR, and the ash was activated and removed by CO_2 to form mesoporous structure. SCFS-AC has a high specific surface area, pore volume and pore size, in which the micropore structure contributes to the specific surface area and provides abundant ion adsorption sites, while mesoporous and macroporous structures reduce the resistance of ion transport and shorten the diffusion distance. Murugan Vinayagam *et al.* [30] further selected a kind of nut shells as raw materials and carbonized them into CO_2 for activation. FE-SEM technology showed disordered channel-like surfaces with pores, and physical activation could also improve the activity of porous carbon materials by forming additional pores inside carbon particles. The material has a specific surface area of 786 m^2/g, a pore volume of 0.212 cm^3/g, and a specific capacitance of 240.8 F/g at 0.2 A/g. It remains at 65.6 F/g at a high current density of 2.0 A/g. The diffusion rate of porous carbon materials using CO_2 as activator is slow, and the activation process is easy to control, but it also leads to a higher activation temperature required, generally between 850 °C and 1100 °C. Moreover, due to the large diameter of carbon dioxide molecules, the pore size distribution is relatively narrow.

Steam is also often selected for physical activation. Porous carbon materials with steam as activator have fast thermal motion, wide pore distribution and uniform pore size, and are easy to operate and environmentally friendly. In the activation process, water vapor is adsorbed on the carbon surface and releases hydrogen and oxygen. The presence of hydrogen prevents the continuous reaction of the active site, and the released oxygen further reacts with carbon monoxide separated from the carbon surface to form carbon dioxide [31]. At the same time, a large number of micropores were produced [32]. Although the detailed mechanism of water vapor activation is still unknown, it is known that the optimum temperature of its activation is 750–900 °C [33]. Within this temperature range, sufficient heat can be guaranteed for the reaction of carbon materials with water vapor, and the water vapor can be uniformly diffused in the carbon. Pundita Ukkakimapan *et al.* [34] took sugarcane leaves as raw material. After carbonization at 500 °C in N_2 atmosphere, ball milling was carried out before steam activation. Due to physical activation, carbon on the surface was removed non-selectively, and the porous structure of the prepared sample was distributed on the surface. However, its higher mesoporous ratio and larger average aperture result in higher specific capacitance. Qin *et al.* [35] used pine nut shell as carbon source to prepare activated carbon through steam activation, and explored the influence of activation temperature, activation time and steam flow rate on sample preparation. Finally, activated at 850 °C for 60 min, the sample prepared with steam flow rate of 18 mL/h had a specific surface area of 956 m^2/g and a mesopol ratio of 37.1%. It has an interconnected layered pore structure.

Although both CO_2 and steam have certain disadvantages as activators alone, they complement each other, and it is not easy to obtain an environment where only steam or CO_2 exists. When biomass raw materials decompose under certain conditions, a certain amount of CO_2 and steam will be produced. Therefore, Mai *et al.* [36] studied the effects of CO_2 and steam activation and co-activation on the physical and chemical properties of activated carbon prepared from linear ferns. Among them, the stems and leaves of linear ferns have a highly porous structure, which is conducive to faster and more uniform dissemination of heat, and have a higher fixed carbon content, which makes it a promising material for preparing biochar. Steam activation produced a higher specific surface area (1015 m^2/g), while CO_2 (653 m^2/g), and both gases alone formed micropores on the carbon. When the steam concentration increased, with the increase of pore formation, only mesopores were observed using steam, because steam stopped the formation of micropores after the early stage of the activation process, and then converted the pores into mesopores by expanding the width of the pores, resulting in a significant decrease in the micropore rate [37]. The combination of CO_2-steam mixed atmosphere and high temperature proved to be a suitable environment to promote the formation of highly porous coke, and proved to adjust the performance of activated carbon by simply adjusting the ratio of water vapor and CO_2. Considering the complexity of the physical activation process, the effects of other factors such as heating rate, activation temperature, activation time or the interaction between them on the performance of activated carbon need to be further studied. Ding *et al.* [38] also used the combination of steam and CO_2 as the activator and apricot shell as the precursor. Firstly, water vapor was injected into the apricot shell for pre-activation, generating abundant micropore structure, which improved the diffusion rate of CO_2, and then CO_2 was injected into the apricot shell for activation. The main chemical reactions that occur are as follows:

$$C + 2H_2O \rightarrow 2H_2 + CO_2 \quad (5)$$

$$CO_2 + C \rightarrow 2CO \quad (6)$$

The obtained samples have high specific surface area and pore volume, and the effective pore volume and mesoporous volume fraction are 0.720 cm^3/g and 55.76%, respectively.

Air as a gaseous oxidant can also be used as an activator for the activation of porous carbon. However, it reacts more positively with carbon, resulting in wear and tear within the pore structure [39], resulting in lower product yield, and requires higher activation temperatures than CO_2 and water vapor when activated by air.

The selection of appropriate activation temperature in physical activation determines whether porous carbon materials can be successfully prepared. The reactions that occur are endothermic reactions. Compared with chemical activation, higher reaction temperature and 2–3 times reaction time are usually required. Although the physical activation method does not require corrosive and expensive chemical reagents as activators, the production cost is low, more environmentally friendly and simple to operate, but it is difficult to accurately adjust the activation process, and the porous structure is relatively disordered. Therefore, in recent years, the study of biomass porous carbon by physical activation methods has become increasingly unpopular.

2.2. Chemical activation

Chemical activation method refers to the reaction of chemical activators (such as sodium hydroxide, potassium hydroxide and phosphoric acid) with raw materials under high temperature conditions. The detachment of carbon atoms and the escape of gas generated by the reaction lead to the formation of abundant pore structures in the activated carbon skeleton. The mechanism of chemical activation and the properties of the product depend largely on the type of activator. The activator mainly dehydrates or erodes the raw materials and then creates pores.

Phosphoric acid is one of the commonly used acid activators, which belongs to a kind of weak acid. The activation step

of phosphoric acid as an activator is mainly divided into two steps. The first step is to depolymerize cellulose, hemicellulose and lignin. and form crosslinking between polymers through dehydration and condensation reaction. Subsequently, phosphate and polyphosphate further cross-linked polymer fragments to form porous structures. It has the advantages of recyclability, low cost and environmental friendliness. Lin *et al.* [40] used sawdust as raw material and used phosphoric acid as activator by one-step carbonization activation method. The addition of phosphoric acid inhibited the formation of tar and protected the carbon skeleton. The prepared porous carbon had rich microporous structure. The optimal carbonization activation temperature was further explored: at 900 °C, the prepared porous carbon has the largest specific surface area (1281.6 m^2/g) and the highest total pore volume (0.638 cm^3/g). Huang *et al.* [41] used pomelo valves as raw material, after simple carbonization, using H_3PO_4 as activator, after hydrothermal activation, the carbonized tissue was composed of a large number of uniform mesopores and micropores, which was conducive to ion transport. The activation of phosphoric acid can promote the formation of thin carbon sheets and porous structures. Under the transmission electron microscope, many 1–3 nm nanopores can be seen, and many amorphous carbon particles with a diameter of about 20 nm are closely connected to effectively promote the diffusion of electrolyte ions. The prepared layered porous carbon electrode has a high specific capacitance of 966.4 F/g at 1 A/g, and has an ultra-high stability of 95.6% even after 10,000 cycles.

Oluwatosin Oginni *et al.* explored the preparation of porous carbon by one-step activation method and two-step activation method respectively. One-step method is to activate the biomass impregnated with activator; the two-step method is to carry out high-temperature carbonization first, and then to carry out high-temperature activation after impregnation and drying in the activator. Compared with the two-step method, its specific surface area is larger and the total pore volume is higher. A large number of micropores and mesopores may be the reason for the high specific capacitance, micropores are also formed on the wall of mesopores [42]. The preparation of porous carbon by two-step activation method can obtain by-products such as charcoal and coke wood liquid, and the overall utilization rate can be improved and the economic efficiency is high. Therefore, Hu *et al.* [43] used lacquer wood as raw material and phosphoric acid as activator to further explore the effects of activation temperature and process. When porous carbon was prepared by one-step method, glycosidic bonds were hydrolyzed due to the impregnation of phosphoric acid and the cracking of aromatic ether bonds in lignin. At the same time, phosphoric acid acts on the organic matter in the precursor to form polyphosphoric acid groups and phosphates, which promotes the precursor to expand into the porous structure together with the acid. It was found that with the increase of activation temperature, the degree of graphitization increased and the conductivity increased. However, when the activation temperature is too high, reaching 800–900 °C, the oxygen-containing functional groups on the surface of porous carbon disappear, resulting in a decrease in the improvement of pore channels and a decrease in specific heat capacity. When the activation temperature is 400 °C, it has the best specific surface area. When the activation temperature is 600 °C, it has a longer discharge time and a larger specific capacitance. Zhao *et al.* [44] used chinar fruit fluffs as raw material and phosphoric acid as activator to explore the optimal activator dose and activation temperature. When 30 wt% H_3PO_4 was selected as the activator, the porous carbon obtained at 600 °C had the best specific surface area of 1758.5 m^2/g, and the porous carbon is mainly mesoporous structure, which can not only reduce the resistance of ion transmission, but also serve as a channel for ion transport. The construction of porous carbon materials with mesoporous structure has research prospects.

In the activation of biomass porous carbon, alkali is commonly used as an activator and KOH is preferred. The activation mechanism is as follow:

$$2KOH \rightarrow K_2O + H_2O \quad (7)$$

$$4KOH + C \rightarrow K_2CO_3 + K_2O + 2H_2 \quad (8)$$

$$C + H_2O \rightarrow CO + H_2 \quad (9)$$

$$CO + H_2O \rightarrow CO_2 + H_2 \quad (10)$$

$$C + 2H_2 \rightarrow CH_4 \quad (11)$$

$$K_2O + CO_2 \rightarrow K_2CO_3 \quad (12)$$

$$K_2O + C \rightarrow 2K + CO \quad (13)$$

$$K_2CO_3 + 2C \rightarrow 2K + 3CO \quad (14)$$

Firstly, KOH dehydrates with carbon and hydrocarbons in raw materials at low temperature. As the reaction proceeds and the temperature rises, the produced H_2O molecules enter the pores of the carbon and further react with water gas to form a small amount of CO, CO_2, H_2 and other gases, and a small amount of CH_4 may also exist. In this process, C atoms are consumed, and a large number of pores are formed when the generated gas molecules escape from the surface of the material. When the temperature reaches 500 °C, the non-carbon elements in the material volatilize and produce tar. When the temperature reaches 600 °C, KOH completely reacts, and K element mainly exists in the form of K_2CO_3 and K_2O. As the temperature continues to increase, K_2CO_3 and K_2O continue to react with C to form K element. When the temperature reaches the boiling point of K element at 723 °C, K element escapes or diffuses into the carbon matrix in the form of vapor. Table 1 summarizes the electrochemical properties of porous carbon electrode prepared by KOH as activator [45–66].

Porous carbon materials were prepared by chemical and physical activation of chestnut seeds with KOH and carbon dioxide at 800 °C. In terms of specific surface area, compared with that before activation (17.1 m^2/g), the specific surface area and total pore volume increased significantly after physical activation (105.7 m^2/g) and chemical activation (1221.2 m^2/g). The pore structure under scanning electron microscope is shown in Figs. 2a–c. Electrochemical analysis results show that the discharge capacitance of chemically activated carbon (173 F/g) is 157% higher than that of CO_2 activated carbon (67.30 F/g) and 3 times higher than that of non-activated carbon (57.4 F/g) at a low current density of 0.1 A/g [67]. Cai *et al.* [45] used cashew nut shells as raw materials, and used KOH as an activator in an argon atmosphere at 850 °C, and activated them after heat treatment in an inert gas flow of 600 °C. After KOH activation, the original hierarchical structure was retained well (Figs. 2d and e). Many new pores appeared in the sample, and the original pore structure was further merged and expanded (Fig. 2f). The specific surface area and pore structure were greatly improved, and the mesoporous amount in the sample increased with the increase of KOH ratio, which was helpful for the diffusion of ions in the electrolyte. The prepared porous carbon exhibits a high specific surface area of 2742 m^2/g and a total pore volume

Table 1
Porous carbon materials prepared by KOH as an activator and their electrochemical performance in supercapacitors.

Carbon source	Specific surface area (m^2/g)	Specific capacitance (F/g)	Electrolyte /Electrode system	Energy density (Wh/kg)	Power density (W/kg)	Type of capacitor (Symmetric/ Asymmetric)	Ref.
Cashew nut husk	2742	305.2 (1 A/g)	6 mol/L KOH/Three electrode	11.2	400	S	[45]
Kapok fibers	3010	144 (0.2 A/g)	1 mol/L $TEABF_4$/PC/Two electrode	33.8	260	S	[46]
Tea	3124	488 (0.5 A/g)	3 mol/L H_2SO_4/Three electrode			S	[47]
Flaxseed residue	3230	369 (0.5 A/g)	6 mol/L KOH/Three electrode	43.5	468.8	S	[48]
Orange-peel wastes	1150	425 (0.5 A/g)	12.0 mol/L $NaNO_3$ (water-in-salt)/Three electrode	36.66	11,500	S	[49]
Egg white	2918	335 (0.5 A/g)	6 mol/L KOH/Three electrode	13.6	300	S	[50]
Ulothrix	2490	324 (1 A/g)	2 mol/L KOH/Two electrode	12.9	800	S	[51]
Castor shell	1527	365 (A/g)	6 mol/L KOH/Three electrode	9.14	500	S	[52]
Osmanthus fragrans	2078.3	351 (0.5 A/g)	3 mol/L KOH/Three electrode	13.86	700	S	[53]
Sorghum	1347	257.2 (1 mV/s)	2 mol/L KOH/Three electrode			S	[54]
Wheat straw	2034.41	286.95 (0.5 A/g)	6 mol/L KOH/Three electrode	8.63	125.15	S	[55]
Helianthus pallet	1510	357 (0.5 A/g)	6 mol/L KOH/Three electrode	25.9	951.4	S	[56]
Wallnut shell	1789.12	262.74 (0.5 A/g)	1 mol/L KOH/Two electrode	7.97	180.8	S	[57]
Corn husk	1370	80 (1 A/g)	1 mol/L $TEABF_4$/AN/Three electrode	20	680	S	[58]
Chestnut	2646	373 (0.5 A/g)	6 mol/L KOH/Three electrode			S	[59]
Areca nut	3723	419 (0.5 A/g)	6 mol/L KOH/Two electrode			S	[60]
Honeysuckle flowers	2582	186 (1 A/g)	$EmimBF_4$/Two electrode	93	954	S	[61]
Ginkgo leaves	2071.8	638.2 (1 A/g)	1 mol/L H_2SO_4/Three electrode	24.8	801.4	A	[62]
Peach gum	1535	406 (0.2 A/g)	1 mol/L H_2SO_4/Three electrode	22.84	400	S	[63]
Quinoa	2597	330 (1 A/g)	6 mol/L KOH/Three electrode	9.5	100	S	[64]
Walnut septum	1003.9	457 (1 A/g)	gel electrolyte (KOH/PVA)/Three electrode	10.12	320	S	[65]
Fatsia japonica seed	870.3	140 (1 A/g)	6 mol/L KOH/Three electrode	23	550	S	[66]

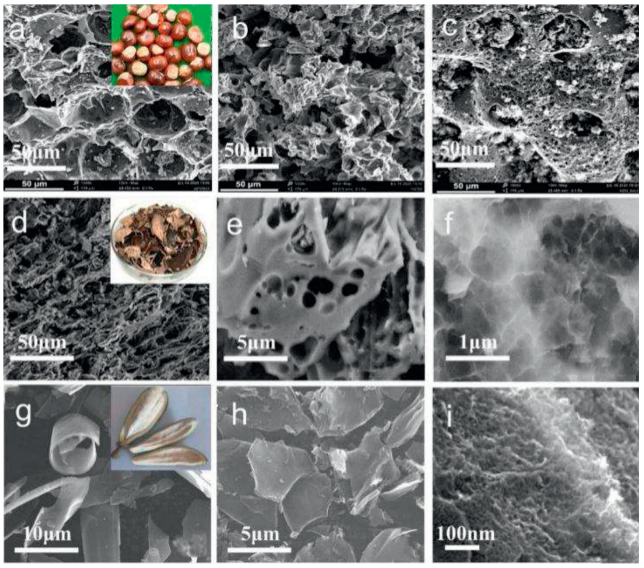

Fig. 2. SEM images of (a) raw biochar and a photograph of chestnut seed (inset), (b) biochar after physical activation, and (c) biochar after chemical activation. Reproduced with permission [67]. Copyright 2020, MDPI. (d-f) SEM images of cashew nut husk biomass-derived porous carbon. Reproduced with permission [45]. Copyright 2019, Elsevier. (g) SEM images of the kapok fibers directly carbonized at 850 °C and a photograph of a broken kapok fruit (inset), and (h, i) the activated kapok fibers with a KOH mass ratio of 2 to the pre-carbonized kapok fibers. Reproduced with permission [46]. Copyright 2019, Elsevier.

of 1.528 cm^3/g. It exhibits a high specific capacitance (305.2 F/g) and good rate capability in a three-electrode system (256 F/g at 20 A/g). Zou *et al.* [46] made the precursor, kapok fiber, and dewaxing through low-temperature pre-carbonization treatment to promote the wettability of subsequent KOH on the carbon precursor, and prepared a carbon sheet with a specific surface area of 3010 m^2/g, a pore volume of 2.756 cm^3/g, and an ultra-high mesoporous volume ratio. The kapok fiber directly carbonized at 850 °C shows a thin-walled tubular structure (Fig. 2g). After carbonization and KOH activation, the tubular fibers break into sheets with a plane size mostly less than 20 μm as shown in Fig. 2h. By observing the surface of the carbon sheet more carefully, the porous structure with abundant nanopores was clearly observed (Fig. 2i). In organic electrolytes, it shows a high specific energy density even at high power. it shows a high specific energy density even at high power. Zhu *et al.* [47] extracted helical carbon fibers from tea by a non-catalytic strategy, and further prepared helical porous activated carbon fibers by KOH activation. The special helical porous structure provides defect sites and high nanoporous rate. Compared with the samples prepared with K_2CO_3 and $ZnCl_2$ as activators, KOH destroyed the graphite crystallite structure in the carbon fiber during the activation process, and the small graphite grains had rich edge positions, which was beneficial to the dispersion of electrolyte ions. The final sample has an ultra-high specific surface area (3124 m^2/g) and pore volume (1.6 m^3/g). The specific capacitance is 488 F/g at 0.5 A/g in the three-electrode system and 187 F/g at 1 A/g in the two-electrode system. Li *et al.* [68] used pine nut shell as raw material. After pre-carbonization treatment, the pre-carbonized sample was mixed with potassium hydroxide and urea in a mass ratio of 1:1:1, and nitrogen atoms were introduced. The sample was activated at a heating rate of 3 °C/min in nitrogen at 600–800 °C. It was found that the specific surface area of the material can be well controlled by controlling the activation temperature. When the temperature is 700 °C, the specific surface area of the material is as high as 2192 m^2/g. When the current density is 0.5 A/g, the specific capacitance is 408 F/g, and after 5000 cycles of testing, the specific capacity retention rate is as high as 95%. The successful doping of nitrogen forms four carbon-nitrogen bonds: pyridine nitrogen, pyrrole nitrogen, graphite nitrogen and nitrogen oxide. The graphite nitrogen atoms are connected to the three carbon atoms in the graphite carbon skeleton, increasing the additional free electrons, thereby increasing the conductivity of the carbon material, because most of the graphite nitrogen atoms are located in the graphite carbon plane, breaking the degree of graphitization; pyridine nitrogen is a nitrogen connected between two carbon atoms on the edge of graphene. It has unhybridized lone pair electrons and strong electron donating ability. Pyrrole nitrogen refers to the nitrogen atom in the five-membered C–N heterocyclic structure of nitrogen-doped carbon materials, which is very unstable. The pyridine and pyrrole nitro-

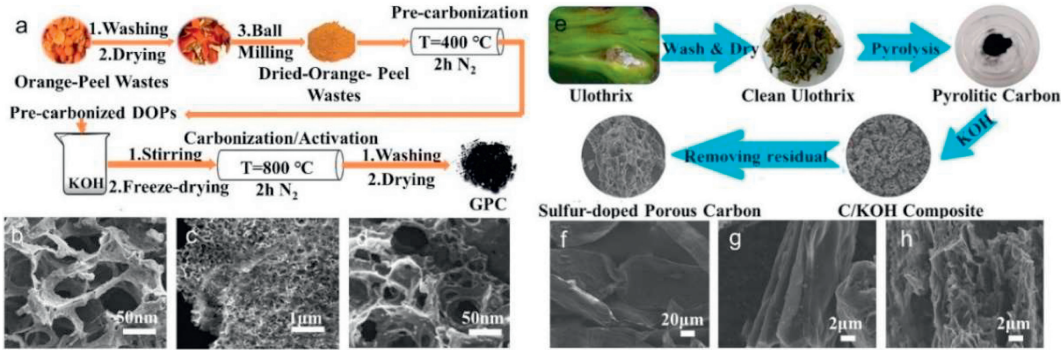

Fig. 3. (a) Schematic illustration of the synthesis pathway for the orange-peel wastes-derived porous carbon. (b-d) SEM images of orange-peel wastes-derived porous carbon. Reproduced with permission [49]. Copyright 2021, Royal Society of Chemistry. (e) Illustration of the synthesis process of biomass-derived sulfur-doping porous carbon. (f–h) SEM images of biomass-derived sulfur-doping porous carbon. Reproduced with permission [51]. Copyright 2022, American Chemical Society.

gen atoms located at the edge of the carbon layer will introduce a large number of surface defects, forming a disordered honeycomb carbon structure, which is more effective in adsorbing heteroatoms and improving electron storage capacity. Li *et al.* [48] used flaxseed residue as raw material. After carbonization in argon atmosphere, KOH was used as an activator, which was used as an excellent activator for micropores. The prepared samples were mainly micropores. The specific surface area was large, up to 3230 m^2/g. More than 70.1% of the micropore volume was contributed by larger micropores (1–2 nm). Large micropores can achieve high charge storage capacity and ensure rapid ion transport, thereby increasing the energy density of supercapacitors without sacrificing high power density. When the current density is 1 A/g, the specific capacitance is 408 F/g, with excellent rate and cycle performance. Even at a high current density of 20 A/g, more than 92.7% of the initial capacitance can be retained. After 10,000 cycles in KOH electrolyte, the capacitance retention rate exceeds 98.1%.

Ceren Karaman *et al.* used orange peel as precursor to carbonize at 400 °C in nitrogen atmosphere, then activated in KOH solution and annealed at 800 °C for 2 h (Fig. 3a). By adjusting the ratio of potassium hydroxide, the porous carbon material with the best electrochemical performance was prepared with the highest specific surface area (1150 m^2/g) and the largest pore volume (991 cm^3/g). When KOH is introduced into waste orange peel as an activator, the synthesized graphene-like porous carbon network exhibits a three-dimensional honeycomb structure composed of interconnected micropores and mesopores (Figs. 3b–d). This unique arrangement essentially prevents the restacking/agglomeration of nanosheets. During the activation process, due to the melting of potassium hydroxide and the cleavage of chemical bonds, the insertion of ions into the carbon layer promotes the formation of an interconnected network. Moreover, due to the catalytic gasification of carbon and the insertion and rapid removal of carbon interlayer ions, the mesoporous structure is likely to be generated [49]. Yang *et al.* [50] used egg white as raw material, which was fully activated in KOH aqueous solution after freeze-drying and carbonization. The etching of KOH led to the formation of a three-dimensional honeycomb structure, which contributed to the full activation of active substances. The prepared material had a large specific surface area (2918 m^2/g), a high specific capacity of 335 F/g in 6 mol/L KOH electrolyte, superior rate performance (240 F/g at 20 A/g) and cycle performance (91.7% capacitance retention after 10,000 cycles). At the same time, it was found that with the continuous increase of potassium hydroxide content, the corrosion performance was enhanced and the pore structure was destroyed. An appropriate amount of KOH as an activator was beneficial to the diffusion of electrolyte ions. Liu *et al.* [51] selected filamentous algae as raw materials, the raw materials are

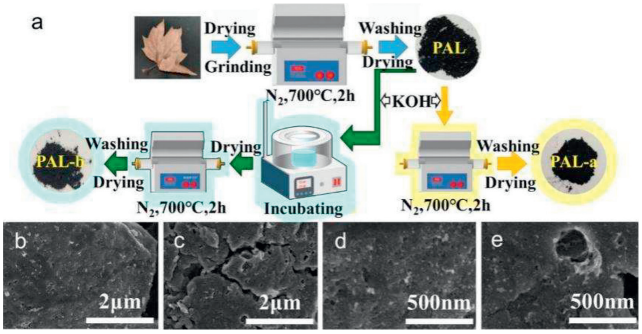

Fig. 4. (a) Diagram of the preparing process for biomass carbon materials from waste *Platanus acerifolia* leaves for supercapacitor. (b–e) SEM images of prepared samples. Reproduced with permission [69]. Copyright 2021, Springer Heidelberg.

filamentous, and the carbon loss is less during the heating process (Fig. 3e), which can better maintain the original morphological map (Figs. 3f and g), and is a high-quality natural template that can be used. The synthesis process of porous carbon is relatively simple. After pyrolysis in an inert atmosphere at 500 °C, KOH was selected for activation without adding additional template material. The samples show many irregular small particles with layered pore structure, and different sizes of pores and channel in Fig. 3h can be found. The specific surface area of the prepared sample is up to 2490 m^2/g, and the optimum ratio of KOH activator to sample is explored. When the mass ratio of sample to KOH powder is 1:2, the prepared porous carbon material has the largest specific capacitance (324 F/g at 1 A/g).

In addition to the type of activator, the activation method and activation conditions are also important. The activation method used for the same activation reagent will affect the electrochemical performance of the prepared electrode material. After conventional carbonization of Alsophila spinulosa leaves, Weng *et al.* [69] mixed with potassium hydroxide and water and incubated in a water bath at 60 °C for 1 h before activation in a tube furnace (Fig. 4a). It can be seen from the SEM (Figs. 4b–e) that after the carbon material is immersed in the potassium hydroxide solution during the incubation heating process, some small potassium hydroxide particles are adsorbed on the surface of the carbon material, which is more conducive to the activation of potassium hydroxide. The samples (Figs. 4c and e) incubated in advance have many silts and small pores, which make the pore structure of the samples richer and promote the increase of pore volume [70], which is conducive to the migration of electrolyte ions. The specific surface area (297.22 m^2/g) of the sample prepared by direct carbonization is very small. The total pore volume (1.1079 cm^3/g) is

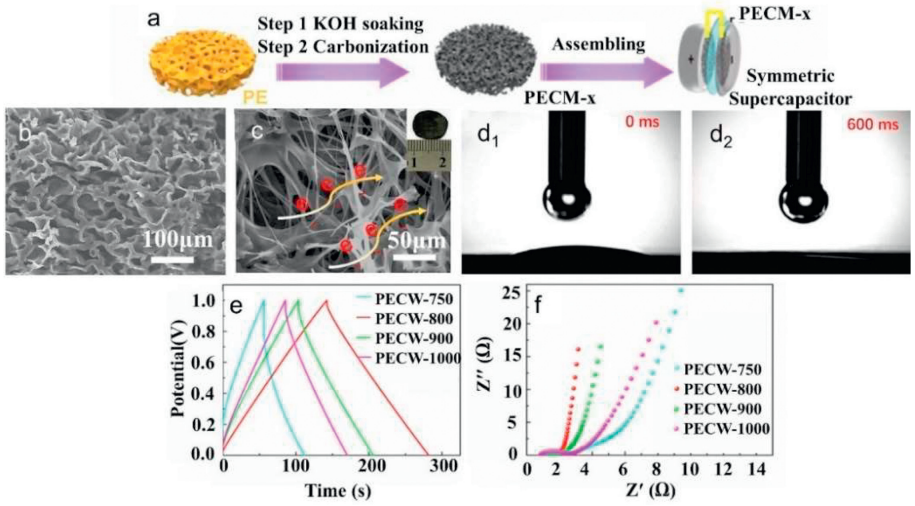

Fig. 5. (a) Schematic diagram illustrating the synthesis of *Pleurotus Eryngii* carbon membrane (PECM) electrode and the assembled PECM-based aqueous symmetric SCs. (b) Side-view SEM images of PECM. (c) Top-view SEM images of PECM-800 electrode. (d_1, d_2) Electrolyte wettability of PECM electrode. (e) GCD curves for PECM-based SCs. (f) Nyquist plots of PECM-based SCs electrode. Reproduced with permission [71]. Copyright 2019, Wiley.

also very small, indicating that direct carbonization cannot obtain the large specific surface area required for the capacitor material. After activation with potassium hydroxide alone, the specific surface area increased to 1766.1 m^2/g, and the specific surface area after incubation heating treatment was higher, reaching 2046.1 m^2/g. More microporous structures can be produced by water bath incubation.

The porous carbon materials prepared above are powder-like, and the powder-like structure limits its development to a certain extent. First, it is necessary to use an additional binder to fix the porous carbon material on the conductive current collector, which reduces the available effective surface area. Secondly, the adhesion of the fixed surface is low, which greatly reduces the cycle stability of the supercharge. Finally, the mass load of the powdered carbon active material coated on the conductive substrate is usually too low to meet the actual demand. Cui *et al.* [71] selected *Pleurotus Eryngii* as a raw material and prepared a three-dimensional heteroatom-doped self-supporting porous carbon film by a two-step pyrolysis method (Fig. 5a). Among them, KOH not only acts as an activator to etch a large number of disordered micropores and mesopores during high-temperature pyrolysis (Figs. 5b and c), but also maintains the original macroscopic structure during the freeze-drying process of KOH-treated slices, which is essential to prevent the initial structure from being destroyed during subsequent pyrolysis. The free-standing carbon film prepared by two-step pyrolysis has a weight loss of 75.1%, indicating that it has high porosity. In addition, various aqueous groups in the electrode give the electrode a higher electrolyte wettability. The wettability test (Figs. 5d_1 and d_2) shows that the electrolyte droplets can quickly diffuse on the electrode surface and quickly enter the pores with a certain contact angle, and also provide additional redox pseudocapacitance sites. The excellent capacitance performance (Figs. 5e and f) of the electrode can be attributed to its large specific surface area, high porosity, and excellent electrolyte wettability. The large specific surface area and high porosity maximize the adsorption of electrolyte ions, and the excellent electrolyte wettability ensures the rapid transport of electrolyte throughout the electrode.

However, the use of KOH as an activator alone will lead to the loss of heteroatoms [72]. In order to improve the electrochemical performance of the electrode, the mixed activation of the two activators is considered. Pan *et al.* first converted dry roses into biochar by simple carbonization. Then, the obtained biochar was activated by a mixture of KOH and KNO_3 under N_2 atmosphere, and the gas by-products such as H_2 and CO were released during the activation process to form a well-organized layered porous structure. The obtained porous carbon material still maintains its original interconnected layered structure after the activation process. The prepared material has a large specific surface area (1980 m^2/g) and good cycle stability. After 140,000 cycles at 100 A/g, the capacitance decay rate is only 4.4% [73]. Su *et al.* [74] used Cattail wool as raw material. Firstly, $Ni(NO_3)_2{\cdot}6H_2O$ was used as activator for pre-activation at 600 °C, and then KOH was used as activator for secondary activation at 800 °C. Under the action of high temperature calcination and KOH chemical activation, the hollow tubular structure becomes brittle, easy to break into short tubes, and the pore structure is less. $Ni(NO_3)_2{\cdot}6H_2O$ was added as activator, and there were abundant pore structures on the surface, which mainly came from the decomposition of $Ni(NO_3)_2{\cdot}6H_2O$:

$$2Ni(NO_3)_2{\cdot}6H_2O \rightarrow 2NiO + 2NO_2 \quad (15)$$

$$NiO + 2HCl \rightarrow NiCl_2 + H_2O \quad (16)$$

When the weight percentage of $Ni(NO_3)_2{\cdot}6H_2O$ is 10%, the capacitance performance is the best. In the three-electrode system, when the current density is 1.0 A/g, it has a high charge storage capacity and a specific capacitance of 314 F/g. In addition, Zhang *et al.* [72] selected KOH and Na_2S co-activation with wheat bran as raw material, and their specific surface area increased (1585.5 m^2/g), pore volume increased (0.977 cm^3/g) and pseudocapacitance contribution increased. The prepared sample has 488 F/g at 1 A/g and good rate performance.

The main components of some biomass raw materials are cellulose, hemicellulose and lignin, and the stability varies greatly under activation. If KOH activation is not enough to etch the stable part, only a few microns of traditional activated carbon particles can be produced. Therefore, Guan *et al.* [68] used melamine and KOH as activators to activate pine nut shells. Melamine will be converted into g-C_3N_4, which is decomposed into NH_3, $C_2N_2^+$, $C_3N_2^+$ and other highly active components, which can effectively etch the stable part. The co-activation of melamine introduces N atom doping, in which pyridine nitrogen and graphite nitrogen

help to accelerate ion transfer. Pyridine nitrogen and pyrrole nitrogen content is higher, accounting for 70%, which can provide additional Faraday capacitance in alkaline solution. Among the prepared samples, although the specific surface area (1847 m^2/g) of the porous carbon material prepared when the mass ratio of pine nut shell, KOH and melamine is 1:3:1 is not the largest, its electrochemical performance is the best due to its high content of pyridine nitrogen and pyrrole nitrogen. The specific capacitance is 324 F/g at 0.05 A/g, and the cycle stability is 94.6% after 1000 cycles at 2 A/g. He *et al.* [75] also used KOH and melamine as dual activators to activate taro stems, and the prepared samples had a higher nitrogen content (4.8%), of which graphite nitrogen content (2.65%) accounted for the largest proportion, followed by pyridine nitrogen (1.61%). The porous carbon material has a high specific capacitance (236.4 F/g at 0.1 A/g) and excellent long cycle durability (89.3% retention after 10,000 cycles at 20 A/g).

In the field of biomass porous carbon activation, apart from acid and base as activators, metal salts as activators have been gradually studied. Commonly used activators are mainly chloride, potassium carbonate, potassium nitrate and so on.

Unlike KOH, $ZnCl_2$ as an activator does not directly react with carbon raw materials, and it mainly removes oxygen by dehydration. The reaction can be divided into three stages according to the temperature: when the temperature is below 327 °C, the oxygen-containing groups in the molecule undergo condensation reaction, accompanied by the breakage of molecular bonds, reducing the number of hydroxymethyl and phenolic hydroxyl groups; when the temperature is 327–700 °C, the intramolecular reaction continues, the molecular structure is rearranged, and the carbon skeleton is initially formed; when the temperature is below 900 °C, small molecules such as methane, formaldehyde, water and CO are generated. At the same time, the impregnation effect of $ZnCl_2$ forms voids between the carbon layers and forms a microporous structure. Ye *et al.* [76] used corn husk as raw material, first carried out hydrothermal carbonization, added potassium salt as catalyst, and then added $ZnCl_2$ as activator to explore the optimal activation temperature. $ZnCl_2$ first reacts with water to form $Zn_2OCl_2{\cdot}2H_2O$. $Zn_2OCl_2{\cdot}2H_2O$ decomposes at high temperature to form $ZnCl_2$ gas and ZnO. $ZnCl_2$ gas escapes to form a large number of mesopores and a small amount of micropores. However, the addition of potassium salt will also change the pore structure. At about 600 °C, $ZnCl_2$ is mainly used as an activator to play a pore-forming role. When the temperature rises to 800 °C, the potassium salt reacts with carbon to form CO_2 and CO, forming a large number of micropores. Feng *et al.* [77] prepared nitrogen and oxygen co-doped porous carbon sheets by one-step carbonization activation method using soybean protein as raw material and $ZnCl_2$ as activator. With the addition of activator, the microstructure of amorphous carbonaceous products changes from irregular bulk particles to flakes. With the increase of zinc chloride content, the porosity of the carbon sheet changes from micropore to layered porous structure, and the addition of $ZnCl_2$ increases the doping rate of nitrogen and oxygen elements. The maximum energy density of the final sample material is 16.27 Wh/kg, and the maximum power density is 8.44 kW/kg.

Considering that $FeCl_3$ is also an effective activator, Mehrnaz Ebrahimi used $FeCl_3$ to activate barley straw. The prepared samples have rich pore structure, and a small part of the porous structure comes from the reaction of $FeCl_3$ and N–O substances in the pre-carbonized samples to form FeOCl and C_3N_4, mainly from the further decomposition of FeOCl. The etching reaction between Fe and carbon will also consume part of the carbon sample, and the resulting carbon iron will produce additional pores after being washed with acid. In a potassium hydroxide electrolyte, the prepared electrode in a three-electrode cell at a current density of 2 A/g. Compared with the porous carbon obtained by traditional $ZnCl_2$ and $FeCl_3$ activation, the following reaction occurs using $CuCl_2$ as an activator [78]:

$$3CuCl_2 + C + 2H_2O \rightarrow Cu + 2CuCl + CO_2 + 4HCl \quad (17)$$

$$4CuCl + C + 2H_2O \rightarrow 4Cu + CO_2 + 4HCl \quad (18)$$

The mild interaction between copper chloride and carbon network caused weak structural damage, resulting in the uniform distribution of worm-like pores on the surface. The prepared layered porous carbon had higher yield, larger specific surface area and more developed pore structure. It has been reported that $CaCl_2$ was used as a biological activator instead of traditional activator to prepare porous carbon materials for ion adsorption. Liu [79] used $CaCl_2$ to activate and crack bagasse in one step, which played a prominent role in improving the specific surface area and pore structure of biomass carbon materials, and introduced abundant nitrogen atoms while creating pores to realize the preparation of nitrogen-rich porous materials. Liu selected urea as the nitrogen source, and had the effect of stretching the carbon layer and expansion. With the increase of temperature, the urea hydrolysis product and $CaCl_2$ fully diffused and filled in the skeleton, and the initial crystal structure of bagasse was destroyed. The highly uniformly dispersed activator aggregates and precipitates to form a crystalline structure $CaCl_2{\cdot}2H_2O$. Finally, the inorganic salts in the pores are removed by repeated washing with hydrochloric acid and water.

Zhong *et al.* [80] considered that Mg and Ca belong to the same group of elements, and using $MgCl_2$ as an activator should also have a good catalytic effect. Therefore, lotus root was used as raw material and $MgCl_2$ was used as an activator. During the reaction, $MgCl_2$ was decomposed to form Mg (OH)Cl, which catalyzes the dehydrogenation, decarboxylation and crosslinking reaction of raw materials. The decomposition of volatile organic compounds can effectively inhibit the coking that may block pores. At temperatures above 500 °C, magnesium chloride is directly decomposed into magnesium oxide, the carbon precursor is further gasified, and the remaining magnesium oxide is used as a template to form a pore structure. The porous carbon material has high specific capacitance and good durability (98% after 10,000 constant charge and discharge cycles in a two-electrode system).

These activators are considered to be toxic chemicals or some require special activation conditions. Complex preparation processes will limit the use of these activators, and some nontoxic activators have attracted attention. Among nontoxic activators, potassium acetate has the advantages of easy availability, low cost, and easy solubility in water and ethanol. In addition, the mild potassium acetate etching also retains the natural structure of the material and does not destroy too many pore structures when activated. Xu *et al.* [81] prepared a layered porous carbon by one-step carbonization method using biomass tar as raw material and potassium acetate as activator. The specific capacitance was as high as 261.7 F/g at 1 A/g, and the capacitance retention rate was 91% after 5000 cycles at 5 A/g, which not only treated the harmful biomass tar inevitably produced in the biomass gasification process. It also provides another solution for the manufacture of supercapacitor electrode materials. Potassium nitrate was selected as an activator instead of a strong corrosive activator. The prepared porous carbon material has a high specific surface area (2400 m^2/g). Potassium benzoate is weakly alkaline and corrosive. As an activator, it can generate a large number of microporous structures and introduce potassium atom doping, Lu *et al.* [82] selected it, used plum shells as carbon precursors, and *N*,*N*'-diphenyl thiourea as nitrogen and sulfur sources to prepare nitrogen–sulfur co-doped porous carbon by one-step method. Doping nitrogen atoms can improve the

wettability of carbon, and the introduction of larger sulfur atoms will lead to more polarized surfaces and defect structures, ensuring a larger specific surface area. The introduction of heteroatoms provides more active sites for reversible redox reactions. At the same time, *N*,*N*'-diphenyl thiourea also played a synergistic activation role in the preparation process. The decomposition of *N*,*N*'-diphenyl thiourea produced some volatile gases and nitrogen and sulfur substances. The emission of volatile gases further promoted the formation of pores. The prepared porous carbon material has excellent wettability, and the specific capacitance is 338 F/g at a current density of 0.5 A/g in 6 mol/L KOH electrolyte. The rate performance is excellent, and the retention rate is 92.3% after 10,000 cycles. As we all know, straw (such as corn, wheat, rice) is widely used in rural areas for cooking, producing hundreds of tons of plant ash every day, often discarded. Considering that plant ash is rich in K^+, Ca^{2+}, Mg^{2+} in the form of oxides or carbonates, Yin *et al.* [83] developed a simple direct heat treatment to prepare porous carbon with seeds as carbon precursor, plant ash as activator, and eggshell (83%–85% calcium carbonate) as hard template. The activation process includes the decomposition of K_2CO_3, the reaction with C and the decomposition of $CaCO_3$. The obtained carbon specific surface area with a high yield of 75% is 343.6 m^2/g, the specific capacitance at 0.5 A/g is 250.5 F/g, and good cycle stability (10,000 cycles, the capacitance retention rate is about 99.0%).

The activated carbon prepared by the mixed activator has more mesopores, macropores and specific surface area than the single activator, and introduces heteroatom doping to a greater extent. The modification of biomass-derived porous biochar by heteroatom doping can significantly improve the capacitance performance. Yuan *et al.* [84] used corn straw as raw material, K_2CO_3 as activator, melamine as nitrogen source, phytic acid as phosphorus source and activator at the same time, etch carbon materials to generate more mesopores and micropores. N and P elements were uniformly doped in the carbon skeleton. The specific surface area of the prepared sample was 1136.31 cm^2/g, and the specific capacitance was 203.5 F/g at 1 A/g current density. After 5000 cycles at 10 A/g current density, the capacitance did not decrease and the cycle stability was good. Kong *et al.* [85] used laver as precursor and $KCl/ZnCl_2$ as composite activator and porogen to prepare carbon materials with high specific surface area (1514.3 m^2/g), three-dimensional interconnected hierarchical porous structure and abundant heteroatom doping. Ning *et al.* [86] prepared porous carbon materials by one-step carbonization reaction using succulent leaves as raw materials, $Mg(NO_3)_2{\cdot}6H_2O$ and zinc chloride as dual activators. The porous carbon material has superior specific surface area (2136.2 m^2/g) and excellent electrochemical performance (specific capacitance of 455.3 F/g at 1 A/g). Using waste tea as raw material, $ZnCl_2$ and $Mg_5(OH)_2(CO_3)_4$ as dual activators, Zhang *et al.* [87] prepared samples with large specific surface area (1968.6 m^2/g) and specific capacitance (321 F/g at 1 A/g). Zhao *et al.* [88] prepared N, P and S co-doped porous carbon materials by one-step simultaneous carbonization and activation using peanut powder as raw material, $ZnCl_2$ and $Mg(NO_3)_2{\cdot}6H_2O$ as dual activators. The specific surface area is 2090 m^2/g, and the total pore volume is 1.42 cm^3/g. Mg salt and $ZnCl_2$ are transformed into metal oxides (MgO and ZnO) under anaerobic high temperature conditions, which are used as double templates. The possible reaction principle is as follows: With the increase of temperature, zinc chloride gradually transforms into zinc oxide as a template, and pores are formed after etching in hydrochloric acid solution. When the temperature rises to 600 °C, as the carbon begins to form, some zinc oxide is further transformed into metal zinc, which is released in the form of steam to generate pores in the carbon skeleton. $Mg_5(OH)_2(CO_3)_4$ is completely transformed into magnesium oxide in the carbon framework. After etching treatment, pores will also be generated. The materials prepared by co-activation are dominated by micropores and rich in mesoporous macroporous structures.

However, the traditional heating device has the problems of uneven heating, long time required and high cost. The emergence of new heating methods solves this series of problems well [89]. Microwave pyrolysis produces a large amount of heat through the electromagnetic oscillation and high-speed movement of molecules [90]. As a novel biomass pretreatment method, it is more energy-saving and efficient. Single microwave-assisted hydrothermal carbonization is not enough to form porous carbon with excellent electrochemical properties. It is usually necessary to further chemically activate with activators and then hydrothermally treat to obtain porous carbon with layered pore structure. Bo *et al.* [91] used biomass waste of camellia oleifera as raw materials. After pre-carbonization at 400 °C, potassium hydroxide was added as an activator and microwave treatment was performed. The carbonized material can absorb microwave radiation and heat up sharply within 2 min. The prepared porous carbon material has a rich pore structure and a large surface area of 1726 m^2/g. Beet pulp is rich in cellulose structure and rich in yield. Emre Gür *et al.* [92] used beet pulp as raw material, citric acid as catalyst, and microwave-assisted hydrothermal treatment at 200 °C to explore the activation effect of Mg $(CH_3COO)_2{\cdot}4H_2O$ and $ZnCl_2$ as activators at 500, 600 and 700 °C, respectively. After dehydration, Mg $(CH_3COO)_2{\cdot}4H_2O$ is converted to magnesium oxide at high temperature. The main reactions are as follows:

$$Mg(CH_3COO)_2{\cdot}4H_2O \rightarrow Mg(OH)CH_3COO + CH_3COOH + 3H_2O \quad (19)$$

$$Mg\ (OH)\ CH_3COO \rightarrow MgO + CH_3COOH \quad (20)$$

The experimental results show that the sample prepared by using $ZnCl_2$ as the activator has a richer mesoporous structure than the sample prepared by using Mg $(CH_3COO)_2{\cdot}4H_2O$. The specific surface area of the prepared porous carbon is up to 950.31 m^2/g. When the activation temperature is 700 °C, the prepared electrode exhibits higher capacitance in alkaline water electrolyte. In 6 mol/L KOH electrolyte, when the current density is 0.5 A/g, the energy density is 16.3 Wh/kg. When the current density is 5 A/g, the power density is 3750.9 W/kg. In addition, the use of ultrasonic assisted is also a new process to reduce the activation temperature and achieve energy saving effect. Under the action of ultrasound, the reactants are uniformly mixed, the diffusion of reactants and products is accelerated, and the solid-liquid multi-phase reaction rate is increased. Zhou *et al.* [93] successfully prepared straw-based porous carbon by microwave-assisted method at 500–700 °C activation temperature with NaOH as activator (Fig. 6a). When the activation temperature is 600 °C, the specific surface area is 1820.2 m^2/g, showing a high specific capacitance (420 F/g at 1.0 A/g). Chen *et al.* [94] proposed a flame combustion carbonization strategy in air, using molten salt flame retardants to prepare biomass-based porous carbon materials. With cotton, dandelion and catkin as precursors and K_2CO_3–KCl molten salt as flame retardant, the carbonization time during flame combustion is only 10 min. In the process of flame combustion carbonization, biomass combustion produces carbon dioxide, water and other gases. The K_2CO_3–KCl and the molten salt liquid obtained by rapid melting of high temperature flame can cover the surface of biochar and prevent it from contacting with air, thus becoming a flame retardant. K_2CO_3–KCl also has the function of activation and template. As the temperature further increases to 800 °C, K_2CO_3 begins to decompose to form KCl molten salt, and the generated CO_2 and K activate carbon. During the combustion carbonization process, due to the short carbonization time, the molten salt will be dispersed into the sample, resulting in uniform pore size (Figs. 6b–d).

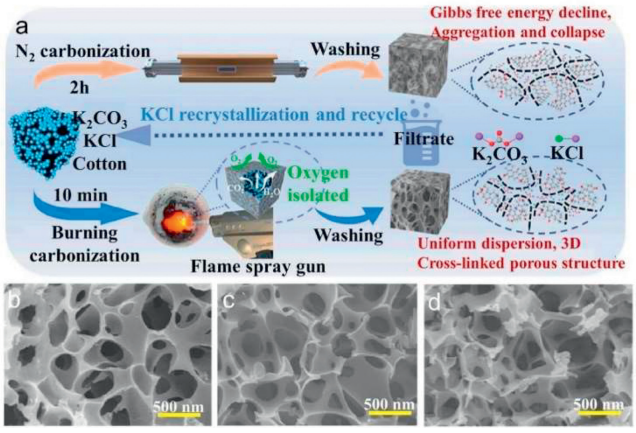

Fig. 6. (a) Preparation process and burning mechanism of FBCT-X and TF-X, and the corresponding processes can be indicated. SEM images of (b) FBC10-Cot, (c) FBC10-Dan, and (d) FBC10-Cat. Reproduced with permission [94]. Copyright 2023, Elsevier.

At the same time, when the carbonization temperature is lower than the melting point of the molten salt, the salt is embedded in the carbon skeleton and can be used as a template to prepare three-dimensional layered porous carbon.

Chemical activation is widely used due to its lower operating temperature, easier operating procedures and adjustable porosity. The activation process requires quantities of chemical substances, and washing after activation also requires a large amount of acid solution, alkali solution and water, and chemical activation is not conducive to the formation of graphite carbon, which limits the conductivity of carbon materials to a certain extent. And chemical activation may introduce excessive functional groups, which reduce electronic conductivity and may be harmful to rate performance and stability. In some cases, chemical activation may lead to uncontrollable pore size distribution [23].

3. Unconventional activation

However, the control of pore size by traditional activation methods is limited, which seriously limits the further development of carbon materials. In order to meet the need for renewable and cheap energy materials, the activation of biomass porous carbon requires some alternative strategies.

3.1. Self-activation method

Studies have shown that some biomass rich in cellulose and potassium and sodium can be directly converted into porous carbon with high specific surface area, without the need for additional activators. gases emitted from water, carbon dioxide or H_2 to the carbon skeleton led to the formation of pores. Chrysanthemum is rich in cellulose and has high potassium and sodium content [95,96]. Zhang *et al.* [97] selected Glebionis coronaria as raw material. Since cellulose and lignin are the main components of xylem vessel cells, lignin is converted into a carbon framework at high temperature, which avoids the complete collapse of the xylem container after carbonization. Cellulose reacts with gases released during pyrolysis/carbonization, such as water, carbon dioxide and H_2, to produce developed porosity. Because the specific surface area of the prepared porous carbon material is 1007 m^2/g, the obtained activated carbon has a high bulk density and rich pseudocapacitive sites. Symmetric supercapacitors have high volumetric specific capacitance and energy density (the maximum values are 264 F/cm^3 and 23.5 Wh/L, respectively). Yang *et al.* [98] selected wild hollyhock as raw materials. After carbonization, the porous tubular transport tissue was still retained, forming a large number of interconnected macroporous and mesoporous porous carbon skeletons. At the same time, due to its high cellulose content, it is self-activated during the carbonization process to form a rich microporous structure, and the prepared material has a high specific surface area (954 m^2/g).

During the carbonization process, the reaction of the carbon skeleton itself will release a large amount of small molecule gases, such as CO_2 and H_2O. Du *et al.* [99] developed a closed pyrolysis method to construct a compact silicon shell closed structure. The resin is used as the precursor to fabricate a hollow carbon sphere with a rich porous structure. The closed and dense silicon shell structure effectively prevents the escape of gas. Using the gas released by the reaction itself as an activator, the prepared porous carbon material exhibits excellent specific capacitance (330 F/g at 0.5 A/g). After 10,000 cycles, the stability is excellent. The initial capacity retention is 88.5%. On this basis, Du *et al.* [100] continued to study the silicon-limited activation method, using microcrystalline cellulose as a carbon precursor, tightly wrapped with a silicon coating, and pyrolyzed in an inert atmosphere. The gas generated by the reaction preferentially stays in the closed pores of the MCC, rather than being released into the atmosphere under the obstruction of the closed space of the dense silica layer, in which CO_2 and H_2O activate the carbon skeleton to form a rich mesoporous structure. The specific surface area of the prepared sample can reach 797 m^2/g, which is 33% higher than that of the limited activation method without silicon coating.

3.2. Bioactivation method

Due to the rich sugar content of biomass itself, the introduction of yeast is considered to develop a green and inexpensive activation process. By introducing yeast, yeast respiratory conversion produces alcohol and releases carbon dioxide to form pore structure. Lian *et al.* [101] used banana peel as raw material, mixed active dry yeast with warm water to activate yeast, pressed banana peel into small pieces and mixed the two materials evenly. The samples were stored in a water bath at 37 °C for 3 h and then carbonized at 900 °C for 1 h in N_2 atmosphere. The prepared sample has a rich pore structure due to yeast respiration, which is dominated by microporous structure. The total specific surface area is 1084 m^2/g, and the micropore specific surface area is 706 m^2/g.

3.3. Template assisted activation method

Conventional physical and chemical activation methods can be used to develop large specific surface area and pore volume, but it is difficult to obtain ordered nanoporous structure. The template carbonization activation strategy can effectively control the morphology and pore size, and can be used to develop pore size and balanced ordered microstructure in the range of 1–200 nm [102]. The template carbonization activation strategy can be divided into two steps. The first is the carbonization of carbon precursors and hard template composites [24]. The hard template includes zeolite, SiO_2, nano-$CaCO_3$, *etc*., and the mesoporous structure is generated by carbonization. The second step is the activation of chemicals such as KOH and NaOH to form microporous structures. Li *et al.* [103] selected boric acid as a new activator, using auricularia as raw material, through soaking, the volume of dried auricularia will expand to 3.5 times the original size, under the action of hygroscopicity, boric acid can enter the interior of auricularia well. During the carbonization process, boric acid first melts into molten Be_2O_3, which has high viscosity and excellent wettability, adheres to the agaric matrix, and then KOH is used to remove the Be_2O_3 template. The prepared material has a typical honeycomb-like porous structure. It contains a large number of mesoporous

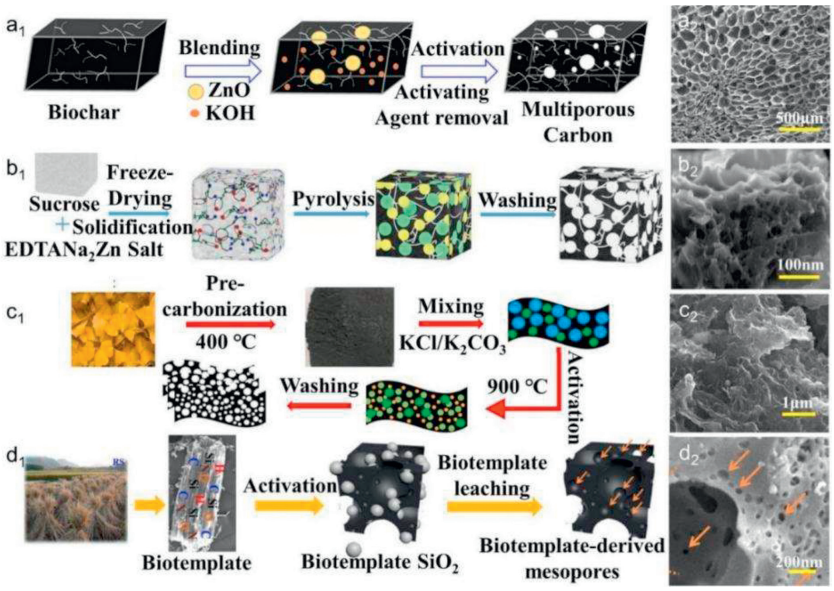

Fig. 7. (a_1) Scheme of the formation mechanism of the mesopore and micropore in the WCS biochar by using ZnO nanoparticles and KOH as activating agents. (a_2) SEM images of the WCS biochar. Reproduced with permission [104]. Copyright 2020, American Chemical Society. (b_1) Schematic diagram for the preparation of nitrogen-doped hierarchical porous carbons. (b_2) SEM images of ESCT samples. Reproduced with permission [105]. Copyright 2019, Elsevier. (c_1) Schematic illustration for the synthesis process of KISPCs. (c_2) FESEM images of KISPC. Reproduced with permission [110]. Copyright 2021, Elsevier. (d_1) Scheme of preparing N-self-doped HPC from RS *via* the self-biotemplating method. (d_2) SEM images of DAC-$KHCO_3$. Reproduced with permission [112]. Copyright 2018, American Chemical Society.

structures, and the specific surface area of the prepared material can reach 2279.5 cm^2/g. Chun-Hsiang Hsu *et al.* [104] used rhombus shells as raw materials, nano-zinc oxide as a template, and KOH as an activator to prepare porous carbon materials with a specific surface area of up to 1537 m^2/g and good electrochemical performance (128 F/g at 5 mV/s). However, nano-zinc oxide can not only be used as a template for the production of mesopores, but also as an activator for the preparation of layered porous carbon (Figs. $7a_1$ and a_2). Wang *et al.* [105] selected $EDTANa_2Zn$ salt as a hard template, activator and nitrogen source at the same time. Sucrose was used as a carbon precursor and $EDTANa_2Zn$ salt was mixed in deionized water. After freeze-drying and curing treatment, a composite material with intertwining structure was obtained. $EDTANa_2Zn$ salt was decomposed to produce zinc oxide and Na_2CO_3 nanoparticles. Na_2CO_3 nanoparticles were used as hard templates. As the carbonization temperature increased, nano-ZnO was used as an activator. It reacts with the carbon material to etch to form a microporous structure. Zn exists in the form of simple substance until 907 °C reaches the boiling point of Zn, leaving small mesopores by evaporation (Fig. $7b_1$). After washing with hydrochloric acid to remove the template, a nitrogen-doped carbon with a layered porous structure was obtained (Fig. $7b_2$). The prepared porous carbon material has the highest specific capacitance of 283 F/g at 0.1 A/g. In addition, it has high specific surface area (2160 m^2/g) and high nitrogen content (1.85%), and has excellent rate performance and cycle durability. Jiang *et al.* [106] used waste straw as raw material and nano-zinc oxide as both template and activator. Nano-zinc oxide has a placeholder effect to produce rich mesoporous structure, and etched carbon atoms at high temperature to form microporous structure. The optimum carbonization temperature was explored through experiments: when the carbonization temperature was 800 °C, the specific surface area of biochar was the highest, reaching 1293.2 m^2/g. Molten metal salts are also often used as templates. Salt templates have lower eutectic points, which can increase the contact area between carbon precursor and activator at low activation temperature, thus greatly improving the utilization efficiency of activator. As an excellent thermochemical medium, it has strong thermal conductivity. The molten salt medium has good reaction ability with impurities (such as silica [107] and potassium oxide [108]) in biomass, and high purity derived carbon is obtained. As a green nontoxic template, chloride can adjust the pore structure and microstructure of carbon materials. Zhang *et al.* [109] prepared porous carbon nanosheets derived from Ginkgo biloba leaves using $CaCl_2$ and KCl molten salts as activators and templates. Calcium chloride has a dual role in the preparation of porous carbon materials. First, the fixed ammonia comes from the decomposition of the ammonia precursor, resulting in high nitrogen content in the synthesized carbon product, on the other hand, calcium chloride can be used as a pore-forming / expansion agent to introduce pores into carbon matrix materials during carbonization, resulting in the formation of pores in the final carbon products. At the same time, potassium chloride can also be used as a template to penetrate into the carbon precursor to form pores. Adjusting the ratio of molten salt is the key to the preparation of porous carbon materials with high porosity. With the increase of KCl ratio, the specific surface area of the prepared carbon materials increases. When the molar ratio of KCl and $CaCl_2$ is 0.75:0.25, the prepared carbon-based supercapacitor exhibits a good specific capacitance of 150.4 F/g at 0.05 A/g. After 10,000 charge and discharge cycles at 1 A/g, it has good cycle performance, capacity retention of 94.2%, and electrochemical performance is the best. On this basis, Zhang *et al.* [110] further prepared N/S co-doped flake porous carbon from Ginkgo biloba leaves by using molten salt KCl/K_2CO_3 as template and activator (Fig. $7c_1$). The main activation effect is chemical/physical activation and carbon lattice expansion caused by K_2CO_3.When KCl is used as a template, Cl-etching carbon skeleton will also form a pore structure (Fig. $7c_2$). The prepared porous carbon material as an electrode has 215.2 F/g at 0.05 A/g and maintains 78.9% at 20 A/g (169.8 F/g at 20 A/g). There is only 1.6% capacity decay after 10,000 charge and discharge cycles. However, although the biomass porous carbon materials produced by template carbonization activation have large surface area and mesoporous structure, most of them are dominated by micropore effect. Although they have high capacitance, their rate performance is poor. Therefore, Hu *et al.* [111] proposed a preparation strategy based on the combination of *in-situ* hard tem-

plate method and NaOH activation. The lotus seed shell was used as the carbon precursor and sodium phytate was used as the hard template precursor, which was fully mixed to form a mixed gel. Soluble sodium phytate was pyrolyzed to nano-$Na_5P_3O_{10}$ during carbonization, and then reacted with NaOH to form nano-Na_2CO_3 and nano-Na_3PO_4 particles, which were uniformly dispersed in the carbon matrix and left mesopores after washing. Combined with the micropores generated by sodium hydroxide activation, a well-developed layered porous carbon with a hollow nest structure was obtained, with a high specific surface area (3188 m^2/g) and a large pore volume (3.20 cm^3/g). Although the prepared porous carbon material has good performance, the preparation process involves the preparation of nano-templates and the complex steps of dispersing in carbon precursors. For rough biomass, the growth structure is compact, the nano-templates cannot penetrate well, and the hard template method is not applicable. Chen *et al.* [112] have noticed that some biomass raw materials contain a large amount of minerals, such as calcium and silicon, which can be used as an internal biological template for *in-situ* mesoporous development. Not only does it not need to introduce additional template substances, but also the biological template is well distributed in the biomass and does not require laborious mixing and dispersion. On this basis, a preparation method combining self-template method and chemical activation was proposed. Rice straw containing a large amount of dispersed silicon (10%–20%) was selected as the raw material, and uniformly dispersed SiO_2 was used as the biological template. When the activator KOH/K_2CO_3 reacts with organic matter at high temperature, the loss of C, H and O leads to the opening of pores. At the same time, SiO_2 particles aggregate into larger particles. The diameter range of these larger silica particles is very wide (Fig. $7d_1$). Removal of these particles will lead to abundant nanopores, and activation will generate a large number of microporous structures (Fig. $7d_2$). The porosity of the prepared samples is reasonable. It allows rapid transport of ions with a large specific surface area and additional pseudocapacitive behavior. As a result, the prepared material has excellent capacitance retention and excellent cycle stability for 357 F/g (0.5 A/g, 1 mol/L H_2SO_4) of the three-electrode system and 260 F/g (1 A/g, 1 mol/L sodium sulfate) of the two-electrode system, which is superior to most biomass-derived carbon. In addition, the energy density is as high as 29.3 Wh/kg at a power density of 900 W/kg.

Although the materials prepared by carbonization and activation have rich pore structures, due to the structural shrinkage caused by the entanglement of natural macromolecules during carbonization, biomass-derived carbon tends to form blocked carbon bodies rather than cavities. The internal space is shielded by the shell, which makes the surface area of ion storage difficult to access and ion transport slow. Opening the internal carbon space is the key to improve the electrochemical performance of biomass-derived carbon. Xue *et al.* [113] prepared porous carbon cages with heavy bio-oil by ice template-assisted activation method (Fig. 8a). The ice crystal is used as a template to grow. By adjusting the volume of the ice crystal, a suitable cavity is formed to prevent the shrinkage of the carbon framework, and the activator is transported to the carbon block to obtain a high accessible surface area (Figs. 8b–d). The obtained porous carbon has an open junction with a cavity and a layered shell.

Although carbonization activation has been successfully used to fabricate porous carbon with mesopores, micropores or layered pores, and these porous carbon electrodes have greatly improved the electrochemical performance of supercapacitors. However, relatively low energy density and rate performance still greatly limit its practical application in the future [114,115]. Balancing the appropriate mesoporous volume and high specific surface area is a major challenge today. Wang *et al.* [116] carried out pre-carbonization and KOH continuous activation of wheat husk

Fig. 8. (a) Schematic illustration of ice template-assisting activation for porous carbon cages. (b) SEM image of PCC-3 (inset: magnified observation). (c, d) TEM images of PCC-3. Reproduced with permission [113]. Copyright 2023, Elsevier.

by chloride salt sealing technology. In the carbonization process, a mixture of potassium chloride and sodium chloride was used as a salt template to form mesopores in the carbon framework. At the same time, the mixed salt can be used as a shielding agent to prevent the carbon framework from oxidizing in the air at high temperatures. The mesopores in the carbon framework can provide active sites for the continuous activation of potassium hydroxide to produce a large number of micropores. Due to the synergistic pore-forming effect of molten salt and potassium hydroxide, the obtained porous carbon exhibits a layered pore structure with a good balance between high specific surface area and mesoporous volume. In a three-electrode system, biomass-derived porous carbon exhibits a high specific weight capacitance of 402 F/g at 1.0 A/g. In a two-electrode symmetric supercapacitor, the biomass-derived porous carbon also provides an excellent specific weight capacitance of 346 F/g at 1.0 A/g, and a good cycle stability of 98.59% after 30,000 cycles at 5.0 A/g.

3.4. Green activator activation

Chemical activation is increasingly challenging due to its associated high corrosivity and toxicity. In addition to these shortcomings, the chemical activation method has a low manufacturing yield, which limits the amplification ability of industrial applications [117]. Therefore, there is an urgent need to adopt greener synthesis strategies based on harmless, non-corrosive activated chemical reagents and sustainable, cost-effective carbon precursors such as biomass-based products and sub-products.

Yan *et al.* [118] found that low-temperature hydrothermal activation is simpler and more energy-saving, in which the wet chemical activation method can introduce abundant heteroatom functional groups while etching the carbon framework. However, the wet chemical activators currently used are mainly corrosive acids (*e.g.*, nitric acid and sulfuric acid) [119]. Therefore, the development of more environmentally friendly wet chemical activators is crucial for customizing the capacitance performance of thick carbon electrodes with high-quality loads. As the substrate of wood-based electrodes, carbonized wood has a unique three-dimensional layered porous structure [120]. Electrons are continuously transmitted through the cell wall, and ions are transmitted along the nanopores in the wood channel. A green, versatile and versatile H_2O_2 hydrothermal activation strategy was reported to prepare linden-derived thick carbon electrodes with ultra-high mass loading (40 mg/cm^2) and excellent capacitance performance (Fig. 9a). The H_2O_2 activation method involves etching and oxidation processes. On the one hand, H_2O_2 molecules begin to

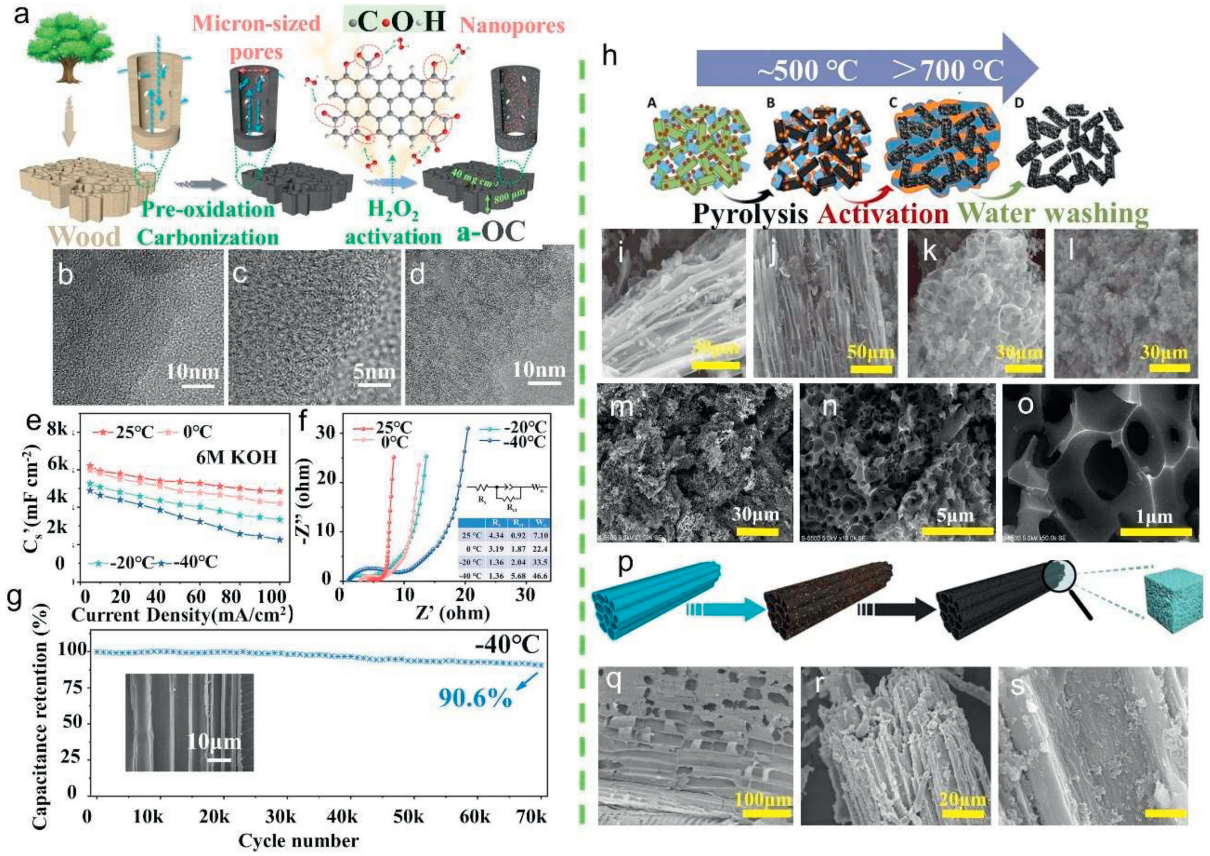

Fig. 9. (a) Schematic illustration of the synthesis process of a-OC materials. HRTEM images of (b, c) OC-900 and (d) a-OC-900, (e) Rate performance and (f) EIS plots of the assembled devices at different temperatures. (g) Long cycling stability of the assembled device over 70,000 cycles under 30 mA/cm^2 at −40 °C. Reproduced with permission [118]. Copyright 2022, Royal Society of Chemistry. (h) Illustration of the synthesis procedure: (A) Blend of the raw materials (sawdust, KCl and $Na_2S_2O_3$). (B) Mixture of the pyrolyzed sawdust with KCl and Na_2SO_4. (C) Porous carbon–KCl–Na_2S monolith. (D) Porous carbon. SEM micrographs of the carbon materials produced from sawdust (i, j) and tannic acid (k, l). Reproduced with permission [126]. Copyright 2019, Elsevier. The surface micrographs of W800–3: (m) 1.5k magnification, (n) 10k magnification, (o) 50k magnifications. Reproduced with permission [127]. Copyright 2021, Elsevier. (p) Morphological evolution process of $KMnO_4$@hemp stem during $KMnO_4$ one-step activation. SEM images of (q, r) the hemp stem and (s) MHPC-1.75 (unwashed). Reproduced with permission [128]. Copyright 2019, American Chemical Society.

etch from the relatively active oxygen-containing carbon atoms and gradually diffuse to the entire carbon base surface, expanding the original nanopores in the carbon skeleton or forming new nanopores, thereby improving the electric double layer capacitance performance of the electrode [121]. On the other hand, the H_2O_2 oxidation process introduces abundant oxygen-containing species to the carbon skeleton, which improves the wettability of the electrode and contributes additional pseudocapacitance. As shown in Figs. 9b–d, the appearance of more nanopores confirms the pore-forming effect of hydrogen peroxide activation. The capacitance performance of the high-load electrode in alkaline (6 mol/L KOH), acidic (1 mol/L H_2SO_4), and neutral (1 mol/L Na_2SO_4) electrolytes was investigated. The electrode has the best performance in 6 mol/L KOH. When the current density is 5 mA/cm^2, the specific capacitance reaches 6205.7 mF/cm^2 (77.6 F/cm^3, 221.6 F/g). When the current density increases to 100 mA/cm^2, the specific capacitance can still maintain 78% of the initial specific capacitance. It can still exhibit excellent capacitance performance under extreme conditions (−40 °C) (Figs. 9e–g). With the rapid development of advanced energy storage devices, not only under normal conditions, but also under extreme conditions, the scope of use is becoming more and more extensive, which brings new challenges to the energy field [122]. Wang *et al.* [123] obtained an ultra-low temperature and high capacity solid-state ZAB|SSE interface without organic solvent by combining the Mn atom cathode with the Zn atom. The prepared water-based ZAB not only provides impressive rate performance and ultra-long discharge life, but also shows good stability in extremely harsh environments. It not only highlights the importance of atomic structure design of oxygen electrocatalysts for ultra-low temperature and large capacity ZABs, but also promotes the development of sustainable energy storage devices under harsh conditions. The (Fe, Co)Se_2@Fe_1/NC composite electrocatalyst prepared by Zheng *et al.* [124] accelerates interfacial electron transfer and reduces energy barriers, showing excellent bifunctional properties. The assembled SS ZABs have high peak power density and good cycle performance at high current density. It also has a certain degree of reliability for mechanical damage (cutting and nail penetration), suggesting its great potential for high safety energy storage under harsh conditions.

Sevilla *et al.* [125] reported a new environmentally friendly synthesis strategy (Fig. 9h), which uses $Na_2S_2O_3$ as an activator and inert salt (KCl) as a suitable reaction medium to produce highly porous carbon based on various biomass products (such as gelatin, sucrose and glucose). The activation process provides a green and sustainable measurement rate for the production of porous carbon, as only affordable and environmentally friendly ingredients are used. The activation process is basically based on the high-temperature redox reaction between carbon-containing substances and sodium sulfate produced by the decomposition of sodium thiosulfate:

$$4Na_2S_2O_3 \rightarrow 3Na_2SO_4 + Na_2S_5 \ (T > 250\,^{\circ}C) \quad (21)$$

$$Na_2SO_4 + C \rightarrow Na_2S + CO/CO_2 \quad (22)$$

The porous carbon particles retain the typical structure of wood, as illustrated by the SEM images shown in Figs. 9i and j. By contrast, when the precursors melt during the heat treatment (*i.e.*, tannic acid melts at around 220 °C and gelatin at <100 °C), the inert solid particles present in the mixture (*i.e.*, KCl and Na_2SO_4) act as templates that direct the formation of a foam-like structure. This morphology is retained by the porous carbon (Figs. 9k and l). It is worth noting that although Na_2SO_4 is the actual activator, when Na_2SO_4 is used instead of $Na_2S_2O_3$, a material with lower pore development is obtained, and it produces lower carbon yield and weaker texture properties. The morphology of carbon particles depends on the melting properties of the raw material. Sevilla *et al.* [126] further extended this synthetic strategy from simple biomass-derived molecules to biomass residues, eucalyptus sawdust, and the resulting porous carbon has a high BET surface area of up to 2600 m^2/g and a large pore volume of up to 2.3 cm^3/g, and a certain amount of sulfur is incorporated into the carbon skeleton during the activation process to achieve sulfur doping.

K_2CO_3 is also commonly used as porous carbon activation because of its low toxicity, low corrosion and very mild. Diego *et al.* [127] found that wasps frequently infested in America, Southeast Asia, Africa and other places caused serious species invasion. They used clay and mud containing different inorganic minerals to build nests. These inorganic and organic components of the honeycomb make it very suitable for the production of activated carbon. Therefore, the honeycomb and K_2CO_3 were used to produce activated carbon at a ratio of 1:3 at 800 °C, and K_2CO_3 was used as an activator to react as Eqs. 13, 14 and 23:

$$K_2CO_3 \rightarrow K_2O + CO_2 \quad (23)$$

The activation of K_2CO_3 promotes the uniform distribution of mesopores and micropores. Some inorganic elements in porous carbon, namely magnesium (6.81%), calcium (3.28%) and silicon (2.25%), can also be used as templates for pore formation in carbon materials to improve the formation of micropores and mesopores (Figs. 9m–o). The specific surface area of the prepared porous carbon material is 765 m^2/g, and the total micropore volume is 0.204 cm^3/g. In a symmetric supercapacitor assembled with an acidic electrolyte using wasp honeycomb activated carbon, the device has better performance than commercial activated carbon, up to 5.33 Wh/kg. The supercapacitor is stable in multiple charge–discharge cycles. After 5000 cycles, the coulomb efficiency is close to 100%, and the capacitance retention rate is 83.6%.

Qiu *et al.* [128] selected hemp stems as raw materials, and their rhizomes have interconnected networks and channels, which provide more sites for the attachment of activators. Potassium permanganate with low melting point and nontoxic was selected as activator (Fig. 9p). Potassium permanganate as activator has the characteristics of gradual activation and mild reaction conditions (400–700 °C). Firstly, $KMnO_3$ is decomposed into K_2MnO_3, MnO_2 and O_2. At about 475 °C, K_2MnO_3 is reduced to K_4MnO_{16}, which is depleted at about 575 °C. The next activation ability mainly comes from the conversion of K_3MnO_4 to $K_4Mn_7O_{16}$. The formation of abundant pore structure (Figs. 9q–s) mainly comes from the etching of carbon skeleton by K_2MnO_4, K_3MnO_4 and K_4MnO_4, forming porous carbon materials with high specific capacitance (255.5 F/g at 1 A/g). Du *et al.* [129] selected carrots as raw materials and Na_2SiO_3 as an activator. In a solvent-free environment, they first grinded and mixed and then washed and etched with water to obtain materials with rich porous structure and high specific surface area. Compared with the porous carbon material with microporous properties prepared by selecting KOH as an activator, it shows better performance in supercapacitors (268 F/g at 1 A/g). Mo *et al.* [130] used the biological medium sodium lignosulfonate as raw material. After freeze-drying, the raw material was subjected to a carbonization activation treatment.

Bamboo is mainly composed of cellulose, hemicellulose and lignin. In order to explore the effects of the three components on the pore structure and electrochemical properties of bamboo chips, Qiu *et al.* [131] used CO_2 catalysis to induce K_2CO_3 green activation strategy to prepare bamboo chips into honeycomb layered porous carbon with excellent supercapacitor performance according to their different components (Fig. 10a). Because hemicellulose is very sensitive to hydrogen ions, it is easy to be broken by acid and difficult to extract. Therefore, wood chips without hemicellulose were selected for comparison. Bamboo chips (debris produced during the production of bamboo chopsticks Fig. $10b_1$), cellulose bamboo chips (extracted from bamboo chips, bright yellow, elastic Fig. $10c_1$), lignin bamboo chips (extracted from bamboo chips, dark brown, irregular, fragile Fig. $10d_1$) and bamboo chips without hemicellulose (Fig. $10e_1$) were selected. After carbonization, the ridge folds and regular vascular bundles on the surface of bamboo chips were retained, and the pore structure was more abundant (Figs. $10b_2$ and b_3). To a large extent, lignocellulosic bamboo chips maintain the original morphology of bamboo chips. However, due to the lack of interaction between hemicellulose and lignin, it is looser than bamboo chips and has more pores (Fig. $10c_2$). After carbonization, it presents a macroporous vascular bundle structure (Fig. $10c_3$). Lignin bamboo chips have lost the morphology of original bamboo chips (Fig. $10d_2$), while bamboo chips lignin carbon (Fig. $10d_3$) is highly porous, quite loose and fragile. Hemicellulose-free bamboo sawdust carbon (BC3) similarly retained the vascular bundle structure of bamboo sawdust (Figs. $10e_2$ and e_3). K_2CO_3 was impregnated at room temperature, and K_2CO_3 was used as an activator to form pores through redox and gas escape. Subsequently, CO_2 was introduced. The addition of CO_2 changed the pore structure of the biomass carbon skeleton. The reaction between CO_2 and carbon was accompanied by the release of CO and the increase of temperature, which promoted the activation of the material surface and further etching to form pores. The specific surface area and porosity of BPC1 (Fig. $10c_4$) are the lowest among the four porous carbons, but its microporosity is very high (80.1%). Cellulose can provide a large number of micropores for BPC. Cellulose carbon (Fig. $10b_4$) and hemicellulose carbon (Fig. $10d_4$) have abundant micropore structures, while lignin carbon (Fig. $10e_4$) has a large number of mesopores and micropores. Compared with other bamboo-derived porous carbon, lignin-derived porous carbon exhibits the best specific capacitance and rate performance, which is mainly attributed to its maximum specific surface area, micropore and mesopore volume. The presence of lignin provides an important guarantee for the excellent specific capacitance and rate performance of porous carbon materials. Cellulose-derived porous carbon exhibits superior cycle stability due to its extraordinary conductivity and stable carbon backbone. Cellulose is the key to determining the excellent cycle stability of the electrode. In addition, the presence of hemicellulose promotes the large specific capacitance, outstanding cycle stability, high energy density and low internal resistance of the electrode to a certain extent. Combining the combined effects of lignin, cellulose and hemicellulose, bamboo-based porous carbon has excellent electrochemical performance. When the current density is 0.5 A/g, the specific capacitance is 253.0 F/g, and the capacity retention is 97.1% after 15,000 charge–discharge cycles.

Li *et al.* [132] used bamboo chips as raw materials, and introduced $K_2C_2O_4$ H_2O and $KHCO_3$ as activators. The introduction of green low-corrosion activators cannot only develop pore structure but also retain the tubular structure inside bamboo chips, which is beneficial to the transfer of adsorbates and ions. The following reaction occurs at about 290 °C (Eqs. 6, 9 and 24):

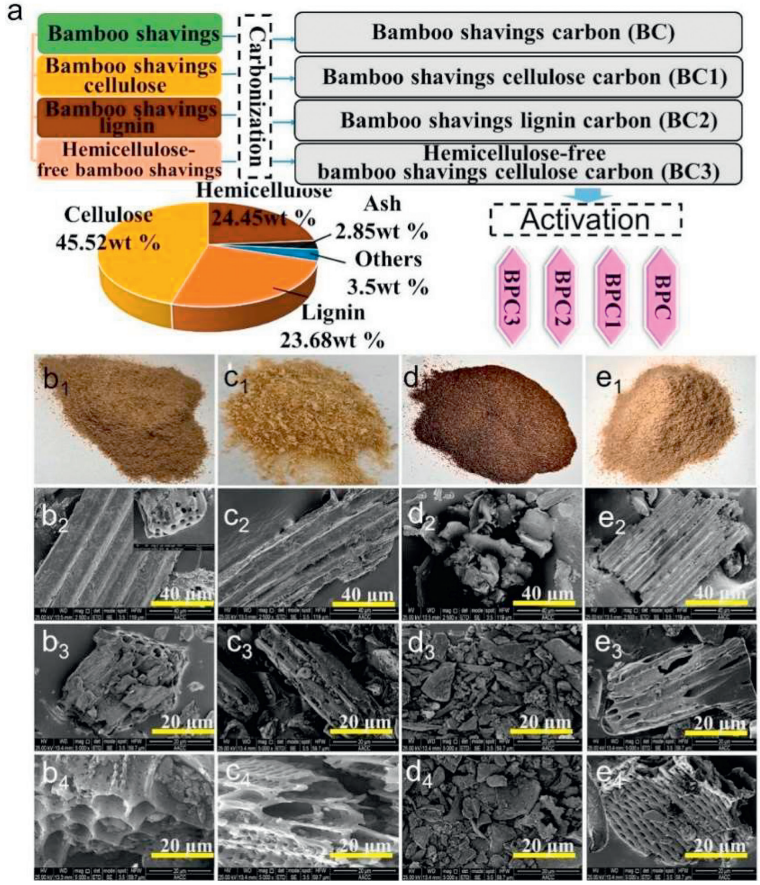

Fig. 10. (a) Process diagram of preparing porous carbon from different components of bamboo shavings. Photographs of (b_1) bamboo shavings, (c_1) bamboo shavings cellulose, (d_1) bamboo shavings lignin, and (e_1) hemicellulose-free bamboo shavings. SEM images of (b_2) bamboo shavings, (c_2) bamboo shavings cellulose, (d_2) bamboo shavings lignin, and (e_2) hemicellulose-free bamboo shavings, (b_3) BC, (c_3) BC1, (d_3) BC2, and (e_3) BC3, (b_4–e_4) BPC, BPC1, BPC2, and BPC3, respectively. Reproduced with permission [131]. Copyright 2022, Elsevier.

$$2KHCO_3 \rightarrow K_2CO_3 + H_2O + CO_2 \quad (24)$$

When the temperature gradually increases, the activation effect is mainly produced by the decomposition of $K_2C_2O_4$:

$$K_2C_2O_4 \rightarrow K_2CO_3 + CO \quad (25)$$

The prepared porous carbon material has a rich pore structure and a specific surface area of 755 m^2/g.

Biomass derivatives also provide new ideas for green activation. Tai *et al.* [21] developed a green physical activation process, using oyster shell powder as an activator, and its main component is $CaCO_3$. CO_2 produced by its thermal decomposition replaces steam, CO_2, air, *etc*, to reduce the cost of physical activation process. The mesopores generated on the surface of the material after physical activation increase the impregnation of the electrolyte and increase the specific surface area. Biomass pyrolysis liquid is the main product of biomass pyrolysis, and its strong acidity limits its utilization. Feng *et al.* [133] proposed a new method for preparing biomass-based activated carbon using biomass pyrolysis liquid as an activator, so that the whole process of activated carbon preparation is realized by biomass. The biomass pyrolysis liquid is mainly composed of bio-oil and wood vinegar. The activation principle is similar to the phosphoric acid activation mechanism in chemical activation. It promotes the bond cleavage reaction while protecting the internal pore structure, and the liquid form can well enter the pores of the raw material to completely activate the material.

Traditional activation has a wide range of applications, but there are some drawbacks. Although the non-traditional activation method is green and energy-saving, it is highly targeted. Table 2 summarizes the electrochemical properties of biomass porous carbon electrodes prepared by different activation methods [30,38,41,69,71,73,74,77–80,86,98,101,104,134–137].

4. Activation of biomass-derived carbon composites for SC electrode materials

The integration of biomass-derived carbon and pseudocapacitive materials (transition metal oxides or hydroxides, conductive polymers, *etc*.) is also a new research direction. Biomass porous carbon-based composites are superior to single-component biochar materials in structure and performance, mainly including (1) biomass carbon / graphene or CNT composites [138], (2) biomass-derived carbon/transition metal oxide or hydroxide composites, and (3) biomass carbon/conductive polymer composites. The pseudocapacitance/biomass porous carbon composite material solves the defects of low specific surface area, weak conductivity, and poor cycle performance of the traditional single pseudocapacitance material. Relying on the sufficient space provided by the carbon material to deposit the pseudocapacitance material, good conductivity promotes charge transfer and improves rate performance and energy density. The robust architecture of biomass-derived carbon can buffer the mechanical stress caused by the Faraday reaction from the pseudocapacitance material during the repeated charging/discharging process, thereby significantly extending the cycle life of the mixture. In the preparation process of the composite material, the hierarchical porous carbon material substrate

Table 2
Electrochemical performance of porous carbon materials activated by different methods.

Carbon source	Activation type	Activation methods	Specific surface area (m^2/g)	Specific capacitance (F/g)	Current density (A/g)	Ref.
Sapindus trifoliatus nut shells	Physical activation	CO_2	786	240.8	0.2	[30]
Coconut shell		Steam	2077	162	1	[134]
Apricot shell		Steam-CO_2 multi-step	2266.433	39.17	0.5	[38]
Sawdust	Chemical activation	H_3PO_4	1281.6	292	0.1	[135]
Waste pomelo valves		H_3PO_4	1432.125	966.4	1	[41]
Platanus acerifolia leaves		Water bath + KOH	2046.1	404	0.5	[69]
Pleurotus eryngii		KOH	583.3	4.6 F/cm^2	10 mA/cm^2	[71]
Rose flower		KNO_3/KOH	1980	350	1	[73]
Cattail wool		$Ni(NO_3)_2{\cdot}6H_2O$/KOH	1581	314	1	[74]
Pine nut shell		Melamine/KOH	2093	324	0.05	[136]
Soybean protein		$ZnCl_2$	1034.33	210.47	0.1	[77]
Wheat straw		$FeCl_3$	257	515	2	[137]
Lotus pollen		$CuCl_2$	1722.5	389.3	1	[78]
Bagasse		$CaCl_2$	945.76	323	1	[79]
Lotus root		$MgCl_2$	877.8	331.8	1	[80]
Succulent-leaf		$Mg(NO_3)_2{\cdot}6H_2O/ZnCl_2$	2136.2	455.3	1	[86]
Hollyhock leaf	Self-activation		954	226	0.5	[98]
Banana peel	Bio-activation	CO_2	1084	172	0.05	[101]
Water caltrop shell	Template-assisted activation	Nano ZnO + KOH	1537	128	1	[104]
Ginkgo biloba leaf		$CaCl_2$/KCl	395.1	150.4	0.05	[109]
Rice straw		Biotemplate + KOH	1909	357	0.5	[83]
Basswood	Green activator activation	H_2O_2	371.6	6205.7 mF/cm^2	5 mA/cm^2	[118]
Wood sawdust		$Na_2S_2O_3$	2600	200	0.5	[126]
Hemp stem		$KMnO_4$	1193	255.5	1	[128]

is established by activation treatment, and the activation type is similar to the biomass porous carbon material. In order to realize the high-value utilization of metal-contaminated plants, Chen *et al.* [139] selected KOH and urea as activators to dissolve metal-contaminated plant in ammonia solution to destroy the chemical bond between cellulose and polysaccharides, and to convert insoluble cellulose into more soluble hydroxyl cellulose, thereby promoting the impregnation of activators. The activation process is divided into three heating procedures. When the temperature is low, urea is decomposed into ammonia gas. Above 700 °C, KOH reacts with carbon, and the synergistic effect of KOH, urea and ammonia water forms a large number of pores on the surface and inside of the carbon. The large surface area (2359.1 m^2/g) and porous structure are conducive to charge storage and rapid ion diffusion, resulting in high capacitance storage and rate performance. Wang *et al.* [140] prepared a carbon substrate with a typical micron/mesoporous/macroporous hierarchical structure by pyrolysis of *Enteromorpha prolifera* and KOH activation. MnO_2 nanostructures were grown by a simple wet chemical reaction process: $4KMnO_4 + 3C + 2H_2SO_4 \rightarrow 4MnO_2 + 3CO_2 + 2K_2SO_4 + 2H_2O$, showing a high specific surface area (2261.1 m^2/g) and a typical hierarchical structure. The hierarchical porous structure can reduce the ion transport resistance and provide a shorter ion diffusion path to promote the electrochemical performance. The birth of some emerging strategies has overcome the problems of high production costs and non-green environmental protection. For example, ultrasonic treatment assisted *in-situ* growth strategy does not involve complex manufacturing processes and any toxic organic solvents [141]. Moreover, ultrasonic treatment promotes the rapid nucleation and controllable growth of layered double hydroxides nanosheets on biomass waste-derived porous carbon surface, with high specific surface area and hierarchical porous structure, which is conducive to exposing more active sites for charge storage [142].

5. Summary and outlook

The pore structure and multi-level distribution largely determine the electrochemical performance of electrode materials, so it is of great significance to summarize the law of activation effect. In this paper, starting from the two aspects of traditional activation and unconventional activation, the activator is used as the starting point to point out the chemical reactions that occur during the activation process, and the complete process of pore formation during the activation process is described. Although biomass porous carbon materials have made considerable progress in the application of various energy storage and conversion, some key issues still need to be solved in the future work (Fig. 11).

(1) Among the existing traditional activation methods, the physical activation method is simple and produces less secondary pollution, but there are problems such as uneven reaction, long-time, high-energy consumption, and difficulty in precise regulation. The obtained activated carbon usually exhibits medium electrochemical performance. Although the chemical activation method has low energy consumption, fast reaction, high efficiency of modified biochar and good pore development, the chemical reagents are often highly corrosive, which is not only unfriendly to the environment but also corrodes a large number of carbon precursors, resulting in low yield of target products. The unconventional activation methods currently developed are highly targeted and do not have universal applicability, and new activation methods need to be developed urgently.
(2) There is still no clear optimal carbonization activation corresponding system for the preparation of biomass porous carbon applied to supercapacitors. For precursors with similar structure composition, the optimal carbonization activation preparation path should be summarized. Although the spe-

Fig. 11. Perspective of biomass-derived porous carbon activation.

cific surface area and pore structure of biochar are closely related, the relationship between them cannot be quantitatively studied, because the differences in the types, properties and carbonization activation methods of biomass will directly affect the correlation between them. The thermochemical conversion process is significantly different, and the accurate synthesis of desired nanostructures faces severe challenges. Even for the same substance, the use of the same activator, different activation conditions or some pre-activation treatment will lead to differences in specific surface area and pore structure. The preparation process of biomass-derived porous carbon materials including carbonization, activation, modification and the key control factors affecting the structure of porous carbon materials still need to be further studied.

(3) The types of biochar materials are complex and diverse, and the surface heteroatom functional groups are various. Considering the establishment of an evaluation database to optimize the selection of biochar greatly reduces the workload of researchers, which will also be the key research direction in the future to screen out excellent biochar materials.

(4) The functionalization of biochar materials is committed to environmentally friendly and cost-effective industrial production methods, which can not only improve the yield of biochar, but also achieve interconnected hierarchical pore structure. The reaction mechanism and process methods of some potential green and industrialized activation treatment technologies need to be further studied.

(5) The interconnection of biomimetic nanostructures is realized by the activation of biomass porous carbon. The porous nature of biomass-derived porous carbon allows the easy and rapid transport of electrolyte ions, which further improves the electrochemical performance. However, the morphology of electrode materials is also important. Naturally inspired nanostructures have been considered to be beneficial structures in widely used electrode materials. The surface area, density and mechanical structure of different surface bionic morphologies will affect the energy storage. For example, the honeycomb structure has uniform and regular pores, excellent mechanical properties, and many active sites. The interconnection of porous carbon structure nanobiomimetic structures through activation steps remains to be studied.

Declaration of competing interest

The authors declare that they have no known competing financial interests or personal relationships that could have appeared to influence the work reported in this paper.

Acknowledgments

This work was financially supported by The Open Fund of Fujian Provincial Key Laboratory of Eco-Industrial Green Technology (No. WYKF-EIGT2022-1), The Open Fund of Key Laboratory of Green Chemical Technology of Fujian Province University (Nos. WYKF-GCT2022-4 and WYKF-GCT2021-1), and Natural Science Foundation of Fujian Province (No. 2020J05220).

References

[1] A. Dimitriadis, S. Bezergianni, Renew. Sust. Energy Rev. 68 (2017) 113–125.
[2] X. Wen, J. Luo, K. Xiang, et al., Chem. Eng. J. 458 (2023) 141381.
[3] W. Deng, Y. Xu, X. Zhang, et al., J. Alloys Compd. 903 (2022) 163824.
[4] W.N. Deng, Y.H. Li, D.F. Xu, et al., Rare Met. 41 (2022) 3432–3445.
[5] T. Wei, N. Zhang, Y. Ji, et al., Chin. Chem. Lett. 33 (2022) 714–729.
[6] G.Z. Chen, Int. Mater. Rev. 62 (2016) 173–202.
[7] H. Yang, S. Ye, J. Zhou, T. Liang, Front. Chem. 7 (2019) 274.
[8] L. Yang, X. Guo, Z. Jin, et al., Nano Today 37 (2021) 101075.
[9] Y. Wang, L. Zhang, H. Hou, et al., J. Mater. Sci. 56 (2021) 173–200.
[10] F. Mao, L. Long, W. Pi, et al., Mater. Chem. Phys. 292 (2022) 126819.
[11] F. Wang, J. Lee, L. Chen, et al., ACS Nano 17 (2023) 8866–8898.
[12] J. Xiao, H. Li, H. Zhang, et al., J. Bioresour. Bioprod. 7 (2022) 245–269.
[13] F. Bilgili, E. Koçak, Ü. Bulut, S. Kuşkaya, Renew. Sust. Energy Rev. 71 (2017) 830–845.
[14] C. Wang, D. Wu, H. Wang, et al., J. Mater. Chem. A 6 (2018) 1244–1254.
[15] F. Wang, L. Chen, H. Li, et al., Chin. Chem. Lett. 31 (2020) 1986–1990.
[16] F. Mao, L. Long, G. Zeng, et al., Diam. Relat. Mater. 130 (2022) 109422.
[17] N. Yang, Y. Zhang, J. Jiang, et al., J. For. Eng. 6 (2021) 89–95.
[18] G. Duan, H. Zhang, C. Zhang, et al., Chin. Chem. Lett. 34 (2023) 108283.
[19] Y. Zhang, H. Gao, X. Song, et al., ChemElectroChem 6 (2019) 5486–5491.
[20] F. Shan, L. Fu, X. Chen, et al., Chin. Chem. Lett. 33 (2022) 2942–2948.
[21] C.H. Hsiao, S. Gupta, C.Y. Lee, N.H. Tai, Appl. Surf. Sci. 610 (2023) 155560.
[22] Y. Qin, Y. Liao, J. Liu, et al., J. For. Eng. 6 (2021) 1–13.
[23] Y. Wang, Q. Qu, S. Gao, et al., Carbon 155 (2019) 706–726.
[24] J. Yin, W. Zhang, N.A. Alhebshi, et al., Small Methods 4 (2020) 1900853.
[25] M. Vijayakumar, A. Bharathi Sankar, D. Sri Rohita, et al., ACS Sustain. Chem. Eng. 7 (2019) 17175–17185.
[26] C.P. Gabrielli, F.A. Kamke, Wood Sci. Technol. 44 (2009) 95–104.
[27] Y.B. Tan, J.M. Lee, J. Mater. Chem. A 1 (2013) 14814.
[28] S. Rawat, T. Boobalan, M. Sathish, et al., Biomass Bioenergy 171 (2023) 106747.
[29] M. Vinayagam, R. Suresh Babu, A. Sivasamy, A.L. Ferreira de Barros, Biomass Bioenergy 143 (2020) 105838.
[30] M. Vinayagam, R. Suresh Babu, A. Sivasamy, A.L.F. de Barros, Carbon Lett. 31 (2021) 1133–1143.
[31] N. Sinan, E. Unur, J. Energy Chem. 26 (2017) 783–789.
[32] Z. Li, D. Guo, Y. Liu, et al., Chem. Eng. J. 397 (2020) 125418.
[33] L. Pan, L. He, Z. Niu, et al., J. Eur. Ceram. Soc. 43 (2023) 612–620.
[34] P. Ukkakimapan, P. Ukakimaparn, T. Wanchaem, et al., Solid State Phenom. 302 (2020) 63–70.
[35] L. Qin, Int. J. Electrochem. Sci. 14 (2019) 8907–8918.
[36] N.T. Mai, M.N. Nguyen, T. Tsubota, et al., Sci. Rep. 11 (2021) 14430.
[37] J. Pallarés, A. González Cencerrado, I. Arauzo, Biomass Bioenergy 115 (2018) 64–73.
[38] Y. Ding, J. Qi, R. Hou, et al., Energy Fuels 36 (2022) 5456–5464.
[39] N. Elboughdiri, B. Azeem, D. Ghernaout, et al., J. Water Reuse Desalin. 11 (2021) 391–409.
[40] M.M. Devi, N. Aggarwal, S. Saravanamurugan, Curr. Green Chem. 7 (2020) 290–303.
[41] J. Huang, J. Chen, Z. Yin, J. Wu, Nanoscale Adv. 2 (2020) 3284–3291.
[42] K. Sahoo, G.L. Hawkins, X.A. Yao, et al., Appl. Energy 182 (2016) 260–273.
[43] S.C. Hu, J. Cheng, W.P. Wang, et al., Renew. Energy 177 (2021) 82–94.
[44] Y. Zhao, J. Yang, X.Y. Wang, X.C. Zheng, J. Mater. Sci. Mater. Electron. 32 (2021) 3498–3511.
[45] K. Januszewicz, A. Cymann-Sachajdak, P. Kazimierski, et al., Materials 13 (2020) 4658.
[46] N. Cai, H. Cheng, H. Jin, et al., J. Electroanal. Chem. 861 (2020) 113933.
[47] Z. Zou, T. Liu, C. Jiang, Mater. Chem. Phys. 223 (2019) 16–23.
[48] S. Zhu, Z. Wang, X. Liu, et al., Ionics 28 (2022) 1129–1141.
[49] J. Li, Int. J. Electrochem. Sci. 15 (2020) 6041–6051.
[50] Y. Li, D. Zhang, Y. Zhang, et al., J. Power Sources 448 (2020) 227396.
[51] C. Karaman, O. Karaman, N. Atar, M.L. Yola, Phys. Chem. Chem. Phys. 23 (2021) 12807–12821.
[52] Y. Zhu, T. Fang, J. Hua, et al., ChemistrySelect 4 (2019) 7358–7365.

[53] S. Liu, K. Chen, Q. Wu, et al., ACS Omega 7 (2022) 10137–10143.
[54] Z. Weng, L. Lu, Y. Ma, et al., Ionics 28 (2021) 697–706.
[55] Z. Liu, D. Tian, F. Shen, et al., J. Power Sources 458 (2020) 228057.
[56] C.A. Okonkwo, T. Lv, W. Hong, et al., J. Alloys Compd. 825 (2020) 154009.
[57] J. Li, Y. Zou, C. Xiang, et al., J. Energy Storage 42 (2021) 103017.
[58] M. Kim, H. Lim, X. Xu, et al., Microporous Mesoporous Mater. 312 (2021) 110757.
[59] C. He, M. Huang, L. Zhao, et al., Sci. Total Environ. 842 (2022) 156905.
[60] A.J.C. Mary, C. Nandhini, A.C. Bose, Mater. Lett. 256 (2019) 126617.
[61] H.h. Fu, L. Chen, H. Gao, et al., Int. J. Hydrog. 45 (2020) 443–451.
[62] M.U. Rani, K. Nanaji, T.N. Rao, A.S. Deshpande, J. Power Sources 471 (2020) 228387.
[63] D. Zhang, L. Sun, Q. Liu, et al., Biomass Bioenergy 153 (2021) 106227.
[64] T.m. Chou, J.L. Hong, Ionics 26 (2019) 1419–1429.
[65] X. Xu, L. Yang, K. Zhuo, et al., J. Energy Storage 41 (2021) 102988.
[66] Y. Bao, H. Xu, P. Chen, et al., New J. Chem. 46 (2022) 14711–14723.
[67] Y. Lin, Z. Chen, C. Yu, W. Zhong, ACS Sustain. Chem. Eng. 7 (2019) 3389–3403.
[68] Y. Sun, J. Xue, S. Dong, et al., J. Mater. Sci. 55 (2020) 5166–5176.
[69] M. Zhou, S.X. Yan, Q. Wang, et al., Rare Met. 41 (2022) 2280–2291.
[70] H. Li, L. Cao, F. Wang, et al., Front. Chem. 8 (2020) 89.
[71] M. Cui, F. Wang, Z. Zhang, S. Min, Int. J. Energy Res. 46 (2021) 4781–4793.
[72] L. Zhang, Y. Wang, S. Yang, et al., Diam. Relat. Mater. 126 (2022) 109061.
[73] A. Khan, R. Arumugam Senthil, J. Pan, et al., Batter. Supercaps 3 (2020) 731–737.
[74] X.L. Su, S. Jiang, G.P. Zheng, et al., J. Mater. Sci. 53 (2018) 9191–9205.
[75] D. He, W. Zhao, P. Li, et al., Appl. Surf. Sci. 465 (2019) 303–312.
[76] G. Ye, Y. Wang, W. Zhu, et al., Chemosphere 298 (2022) 134248.
[77] L. Feng, B. Yan, J. Zheng, et al., New J. Chem. 46 (2022) 10844–10853.
[78] L. Wan, J. Hu, J. Liu, et al., J. Alloys Compd. 859 (2021) 158390.
[79] J. Liu, Y. Deng, X. Li, L. Wang, ACS Sustain. Chem. Eng. 4 (2015) 177–187.
[80] G. Zhong, S. Xu, J. Chao, et al., Ind. Eng. Chem. Res. 59 (2020) 21756–21767.
[81] Q. Xu, X. Ni, S. Chen, et al., Int. J. Hydrog. Energy 14 (2023) 25635–25644.
[82] K.L. Lu, X. Wei, F.-Z. Mao, et al., New J. Chem. 47 (2022) 1247–1255.
[83] Q. Yin, X. Li, X. Yong, et al., Diam. Relat. Mater. 134 (2023) 109798.
[84] X. Yuan, J. Xiao, M. Yılmaz, et al., Sep. Purif. Technol. 299 (2022) 121719.
[85] S. Kong, X. Xiang, B. Jin, et al., Nanomaterials 12 (2022) 1720.
[86] K. Ning, G. Zhao, H. Liu, et al., Diam. Relat. Mater. 126 (2022) 109080.
[87] L. Zhang, G. Zhao, Y. Li, G. Zhu, Ionics 27 (2021) 3195–3205.
[88] G. Zhao, Y. Li, G. Zhu, et al., ACS Sustain. Chem. Eng. 7 (2019) 12052–12060.
[89] S.M. Villota, H. Lei, E. Villota, et al., ACS Omega 4 (2019) 7088–7095.
[90] S.M. Selvam, B. Paramasivan, Chemosphere 286 (2022) 131631.
[91] X. Bo, K. Xiang, Y. Zhang, et al., J. Energy Chem. 39 (2019) 1–7.
[92] E. Gür, T.G. Semerci, F. Semerci, J. Energy Storage 51 (2022) 104363.
[93] G. Zhou, J. Yin, Z. Sun, et al., RSC Adv. 10 (2020) 3246–3255.
[94] B. Chen, D. Wu, T. Wang, et al., Chem. Eng. J. 462 (2023) 142163.
[95] C. Bommier, R. Xu, W. Wang, et al., Nano Energy 13 (2015) 709–717.
[96] P. Kleszyk, P. Ratajczak, P. Skowron, et al., Carbon 81 (2015) 148–157.
[97] Z. Zhang, J. He, X. Tang, et al., Carbon Lett. 29 (2019) 585–594.
[98] B. Yang, D. Zhang, J. He, et al., Carbon Lett. 30 (2020) 709–719.
[99] J. Du, L. Liu, Y. Yu, et al., J. Mater. Chem. A 7 (2019) 1038–1044.
[100] J. Du, H. Lv, Y. Zhang, A. Chen, ChemElectroChem 8 (2021) 2028–2033.
[101] Y.M. Lian, M. Ni, L. Zhou, et al., Chem 24 (2018) 18068–18074.
[102] C. Wang, B. Yan, J. Zheng, et al., Adv. Powder. Technol. 1 (2022) 100018.
[103] D. Li, Y. Huang, C. Yu, et al., Diam. Relat. Mater. 130 (2022) 109432.
[104] C.H. Hsu, Z.B. Pan, C.R. Chen, et al., ACS Omega 5 (2020) 10626–10632.
[105] L. Wang, Q. Zhu, J. Zhao, et al., Microporous Mesoporous Mater. 279 (2019) 439–445.
[106] B. Jiang, L. Cao, Q. Yuan, et al., Materials 15 (2022) 924.
[107] L. He, L. Pan, W. Zhou, et al., J. Eur. Ceram. Soc. 43 (2023) 4114–4123.
[108] S.J. Kim, B.C. Bai, M.I. Kim, Y.S. Lee, Carbon Lett. 30 (2020) 585–591.
[109] W. Zhang, M. Lin, R. Cheng, et al., Diam. Relat. Mater. 113 (2021) 108278.
[110] H. Tian, Q. Fang, R. Cheng, et al., Colloids Surf. A 614 (2021) 126172.
[111] L. Hu, Q. Zhu, Q. Wu, et al., ACS Sustain. Chem. Eng. 6 (2018) 13949–13959.
[112] Z. Chen, H. Zhuo, Y. Hu, et al., ACS Sustain. Chem. Eng. 6 (2018) 7138–7150.
[113] B. Xue, J. Xu, R. Xiao, Chem. Eng. J. 454 (2023) 140192.
[114] X. Liu, S. Zhang, X. Wen, et al., Sci. Rep. 10 (2020) 3518.
[115] Z. Li, Z. Bai, H. Mi, et al., ACS Sustain. Chem. Eng. 7 (2019) 13127–13135.
[116] Y. Wang, Y. Chen, H. Zhao, et al., Nanomaterials 12 (2022) 3804.
[117] A. Borenstein, O. Hanna, R. Attias, et al., J. Mater. Chem. A 5 (2017) 12653–12672.
[118] B. Yan, L. Feng, J. Zheng, et al., Inorg. Chem. Front. 9 (2022) 6108–6123.
[119] W. Song, Z. Zhang, P. Wan, et al., J. Solid State Electrochem. 24 (2020) 761–770.
[120] Y. Chen, Q. Zhang, M. Chi, et al., J. For. Eng. 7 (2022) 127–135.
[121] H. Sun, L. Mei, J. Liang, et al., Science 356 (2017) 599–604.
[122] M. Chen, Y. Zhang, G. Xing, et al., Energy Environ. Sci. 14 (2021) 3323–3351.
[123] Q. Wang, Y. Tan, S. Tang, et al., ACS Nano 17 (2023) 9565–9574.
[124] H. Zheng, S. Wang, S. Liu, et al., Adv. Funct. Mater. 24 (2023) 2300815.
[125] A.B. Fuertes, G.A. Ferrero, N. Diez, M. Sevilla, ACS Sustain, Chem. Eng. 6 (2018) 16323–16331.
[126] M. Sevilla, N. Diez, G.A. Ferrero, A.B. Fuertes, Energy Storage Mater. 18 (2019) 356–365.
[127] D.R. Lobato Peralta, R. Amaro, D.M. Arias, et al., J. Electroanal. Chem. 901 (2021) 115777.
[128] D. Qiu, C. Kang, A. Gao, et al., ACS Sustain. Chem. Eng. 7 (2019) 14629–14638.
[129] J. Du, Y. Zhang, H. Lv, A. Chen, J. Alloys Compd. 853 (2021) 157091.
[130] L. Mo, S. Jia, S. Lin, et al., Int. J. Energy Res. 46 (2021) 2373–2384.
[131] G. Qiu, Z. Miao, Y. Guo, et al., Colloids Surf. A 650 (2022) 129575.
[132] Y. Li, Z. Li, B. Xing, et al., J. Anal. Appl. Pyrolysis 155 (2021) 105072.
[133] P. Feng, J. Li, H. Wang, Z. Xu, ACS Omega 5 (2020) 24064–24072.
[134] C.M. Ashraf, K.M. Anilkumar, B. Jinisha, et al., J. Electrochem. Soc. 165 (2018) A900–A909.
[135] G. Lin, Q. Wang, X. Yang, et al., RSC Adv. 10 (2020) 17768–17776.
[136] L. Guan, L. Pan, T. Peng, et al., ACS Sustain. Chem. Eng. 7 (2019) 8405–8412.
[137] M. Ebrahimi, H. Hosseini-Monfared, M. Javanbakht, F. Mahdi, Biomass Convers. Biorefin. 5 (2023) 2190.
[138] F. Mao, X. Fan, L. Long, et al., Ceram. Int. 49 (2023) 16924–16931.
[139] Z. Chen, M. Zhang, Y. Wang, et al., Green Energy Environ. 6 (2021) 929–937.
[140] X. Wang, S. Chen, D. Li, et al., ACS Sustain. Chem. Eng. 6 (2017) 633–641.
[141] Y. Wang, Y. Liu, Z. Chen, et al., Green Chem. Eng. 3 (2022) 55–63.
[142] Y. Wang, Z. Chen, M. Zhang, et al., Green Energy Environ. 7 (2022) 1053–1061.